

DETECTION OF NITRITE BY THREAD-BASED AND PAPER-BASED DEVICES BY
MODIFIED GRIESS REAGENT



A Dissertation Submitted in Partial Fulfillment of the Requirements
for the Degree of Doctor of Philosophy in Chemistry

Department of Chemistry

FACULTY OF SCIENCE

Chulalongkorn University

Academic Year 2019

Copyright of Chulalongkorn University

การตรวจวัดไนโตรดโดยอุปกรณ์ฐานเส้นด้ายและฐานกระดาษด้วยกรีส์รีเอเจนต์ดัดแปร



วิทยานิพนธ์นี้เป็นส่วนหนึ่งของการศึกษาตามหลักสูตรปริญญาวิทยาศาสตรดุษฎีบัณฑิต

สาขาวิชาเคมี ภาควิชาเคมี

คณะวิทยาศาสตร์ จุฬาลงกรณ์มหาวิทยาลัย

ปีการศึกษา 2562

ลิขสิทธิ์ของจุฬาลงกรณ์มหาวิทยาลัย

พิชชา สิงห์พันธุ์ : การตรวจวัดไนไตรต์โดยอุปกรณ์ฐานเส้นด้ายและฐานกระดาษด้วยกรีสส์รีเอเจนต์ดัดแปร. (DETECTION OF NITRITE BY THREAD-BASED AND PAPER-BASED DEVICES BY MODIFIED GRIESS REAGENT) อ.ที่ปรึกษาหลัก : รศ. ดร.เฟื่องฟ้า อุ่นอบ

พัฒนาอุปกรณ์ตรวจวัดฐานเส้นด้ายและอุปกรณ์ตรวจวัดฐานกระดาษชนิดใหม่สำหรับการตรวจวัดไนไตรต์ด้วยกรีสส์รีเอเจนต์ดัดแปร ทำการดัดแปรทางเคมีของพื้นผิววัสดุด้วยหมู่พาราอะมิโนเบนโซอิลและใช้กรดโครโมโทรปิกเป็นรีเอเจนต์คู่ควบ ได้ทำการยืนยันผลการเติมหมู่ฟังก์ชันบนวัสดุด้วยเทคนิครามานสเปกโทรสโกปี สำหรับการใช้อุปกรณ์ตรวจวัดฐานเส้นด้าย สามารถทำการตรวจวัดไนไตรต์ได้จากการวัดความยาวของแถบสปีบนเส้นด้าย โดยความเข้มข้นที่เหมาะสมที่สุดของกรดโครโมโทรปิก คือ 5 มิลลิโมลาร์ ในสารละลายของกรดซัลฟิวริกเข้มข้น 0.10 โมลาร์และกรดซिटริกเข้มข้น 0.2 โมลาร์ เมื่อใช้สารตัวอย่างปริมาตร 15 ไมโครลิตร พบว่า ช่วงการใช้งานของอุปกรณ์ คือ 50 ถึง 1,000 ไมโครโมลาร์ และความเข้มข้นต่ำสุดที่สามารถสังเกตเห็นสปีบนเส้นด้ายได้ คือ 25 ไมโครโมลาร์ ทำการตรวจสอบความแม่นยำของวิธีการวิเคราะห์โดยพิจารณาจากค่าการได้กลับของไนไตรต์ที่เติมลงในสารตัวอย่าง พบว่า มีค่าร้อยละการได้กลับในช่วง 92.4 – 115.4 สำหรับการใช้อุปกรณ์ตรวจวัดฐานกระดาษ สามารถทำการตรวจวัดไนไตรต์ได้จากการวัดความเข้มสปีบนกระดาษ โดยความเข้มข้นที่เหมาะสมที่สุดของกรดซิทริกและกรดโครโมโทรปิก คือ 0.20 โมลาร์ และ 100 ไมโครโมลาร์ ตามลำดับ และใช้เวลาในการสกัด 15 นาที เมื่อใช้สารตัวอย่างปริมาตร 3.00 มิลลิลิตร พบว่าช่วงการใช้งานของอุปกรณ์ คือ 0.5 ถึง 20 ไมโครโมลาร์ และขีดจำกัดในการตรวจพบและขีดจำกัดในการตรวจวัดเชิงปริมาณ คือ 0.44 และ 1.47 ไมโครโมลาร์ ตามลำดับ ร้อยละการได้กลับอยู่ในช่วง 81.3 – 103.5 เมื่อเปรียบเทียบผลการวิเคราะห์ระหว่างวิธีการดังกล่าวกับวิธีการตรวจวิเคราะห์ด้วยไอออนโครมาโทกราฟี พบว่าค่าการได้กลับและค่าร้อยละการเบี่ยงเบนมาตรฐานสัมพัทธ์ของผลการวิเคราะห์ที่ได้จากวิธีการที่นำเสนออยู่ในช่วงที่ยอมรับได้

CHULALONGKORN UNIVERSITY

สาขาวิชา เคมี
ปีการศึกษา 2562

ลายมือชื่อนิสิต
ลายมือชื่อ อ.ที่ปรึกษาหลัก

5772831023 : MAJOR CHEMISTRY

KEYWORD: NITRITE, MODIFIED GRIESS REAGENT, THREAD-BASED DEVICE, LENGTH-BASED DETECTION, PAPER-BASED DEVICE, COLORIMETRIC DETECTION

Pitcha Singhaphan : DETECTION OF NITRITE BY THREAD-BASED AND PAPER-BASED DEVICES BY MODIFIED GRIESS REAGENT. Advisor: Assoc. Prof. FUANGFA UNOB, Ph.D.

New thread-based and paper-based devices for the determination of nitrite ions based on modified Griess reagent were developed. The surface of the materials was chemically modified with *p*-aminobenzoyl moiety and chromotropic acid was used as a coupling reagent. The functionalization of the materials was confirmed by Raman spectroscopy. By using the thread-based device, the detection of nitrite was achieved by measuring the color band length. The optimum concentration of chromotropic acid was 5 mM in 0.10 M sulfuric acid mixed with 0.2 M citric acid. The working range was from 50 to 1,000 μ M with a sample volume of 15 μ L, where the lowest concentration that produced observable color on the thread was 25 μ M. The recoveries using the spiked samples were in the range of 92.4 – 115.4 %. By using the paper-based device, the detection of nitrite was achieved by measuring the color intensity. The optimum concentration of citric acid and chromotropic acid was 0.20 M and 100 μ M, respectively with 15-minute extraction. The working range was from 0.5 to 20 μ M with a sample volume of 3.00 mL, where LOD and LOQ were 0.44 μ M and 1.47 μ M, respectively. The recoveries using the spike samples were in the range of 81.3 – 103.5 %. When the results of the sample analysis by the proposed methods were compared to those by the ion chromatography method, it was found that the recoveries and RSD of the results obtained from the proposed methods were in acceptable ranges.

Field of Study: Chemistry

Student's Signature

Academic Year: 2019

Advisor's Signature

ACKNOWLEDGEMENTS

This dissertation would not completely succeed without my advisor, Associate Professor Dr.Fuangfa Unob. I would like to express my appreciation for her sincere carefulness, priceless advice, and valuable suggestion during the time of the dissertation. Moreover, I am grateful to Associate Professor Dr.Vudhichai Parasuk; Associate Professor Dr.Pakorn Varanusupakul; Associate Professor Dr.Pattara Thiraphibundet; and Assistant Professor Dr.Wijitar Dungchai for their valuable comments as dissertation committee.

I would like to present my gratefulness to Associate Professor Dr.Wanlapa Aeungmaitripirom; Associate Professor Dr.Apichat Imyim; and Assistant Professor Dr.Aroonsiri Shitangkoon for their suggestions and assistance. Next, I would like to thank all Environmental Analysis Research Unit (EARU) members, especially, Miss Supacha Wirojsaengthong; Miss Petrada Chunnuan; Mr.Theeradit Phothitontimongkol; and Miss Patita Salee for their advice, helps, and encouragement. In addition, I would like to thank Mr.Pitak Niyom; Mr.Suriya Suparnorn; Miss Naraphorn Tunghathaihip; and Mr.Kraisorn Hongchabok for their kind support.

Besides, I am grateful to Assistant Professor Dr.Prompong Pienpinijtham for his help in the sample analysis by Raman spectroscopy and result interpretation. Additionally, I would like to thank Professor Dr.Orawan Chailapakul for the screen-printing device and Professor Dr.Supawan Tantayanon for chemical. My sincere thanks also go to Dr.Waleed Alahmad; Dr.Kanokthorn Boonkitpatarakul; Dr.Waroton Paisuwan; and Miss Kamonwan Meesuwan for suggestions.

This research has been financially supported by the Development and Promotion of Science and Technology Talents Project (DPST).

Finally, I am appreciated to my beloved family for always supporting and encouraging me all through.

Pitcha Singhaphan

TABLE OF CONTENTS

	Page
ABSTRACT (THAI).....	iii
ABSTRACT (ENGLISH).....	iv
ACKNOWLEDGEMENTS.....	v
TABLE OF CONTENTS.....	vi
LIST OF TABLES.....	ix
LIST OF FIGURES.....	x
CHAPTER I INTRODUCTION.....	1
1.1 Statement of the problem.....	1
1.2 Objective of the research.....	2
1.3 Scope of the research.....	2
CHAPTER II THEORY AND LITERATURE REVIEW.....	3
2.1 Nitrite.....	3
2.2 Diazotization reaction and Griess reaction.....	4
2.3 Thread-based and paper-based devices for the determination of nitrite.....	7
CHAPTER III EXPERIMENTAL.....	12
3.1 Analytical instruments.....	12
3.2 Chemicals.....	13
3.3 Determination of nitrite by thread-based platform.....	14
3.3.1 Synthesis of modified cellulose thread and characterization.....	14
3.3.2 Determination of nitrite by the thread platform.....	15
3.3.3 Real samples analysis.....	16

3.4 Determination of nitrite by paper-based platform	17
3.4.1 Synthesis of modified cellulose paper and characterization	17
3.4.2 Determination of nitrite by the paper platform	17
3.4.3 Real samples analysis	19
CHAPTER IV RESULTS AND DISCUSSION	20
4.1 Determination of nitrite by thread-based platform.....	20
4.1.1 Characterization	20
4.1.2 Effect of chromotropic acid and sulfuric acid concentration	25
4.1.3 Effect of sample volume.....	27
4.1.4 Effect of citric acid addition.....	29
4.1.5 Interference studies.....	30
4.1.6 Method validation and sample analysis	31
4.2 Determination of nitrite by paper-based platform	36
4.2.1 Characterization	36
4.2.2 Effect of <i>p</i> -nitrobenzoyl chloride concentration.....	39
4.2.3 Effect of citric acid concentration	40
4.2.4 Effect of sample volume.....	43
4.2.5 Effect of extraction time.....	45
4.2.6 Effect of chromotropic acid concentration	47
4.2.7 Interference studies.....	49
4.2.8 Method validation and sample analysis	50
4.3 Comparison of Method Performance	54
CHAPTER V CONCLUSIONS.....	58
5.1 Conclusions.....	58

5.2 Suggestions for future work 59

REFERENCES 60

VITA..... 66



LIST OF TABLES

	Page
Table 2.1 The maximum permitted levels for nitrite in drinking water, tap water, and food in Thailand.....	4
Table 3.1 Instrument list.....	12
Table 3.2 Chemicals list.....	13
Table 4.1 Wavenumber and Raman band assignments for thread materials	24
Table 4.2 The tolerance limit of interference species in the detection of 75 μM nitrite	30
Table 4.3 Sample analysis and recovery percentage of spiked samples determined by the thread-based platform	34
Table 4.4 Acceptable values of analyte recovery and precision (%RSD) for the determination of analyte at different concentrations	35
Table 4.5 Wavenumber and Raman band assignments for paper materials.....	38
Table 4.6 The tolerance limit of interference ions in the detection of 5 μM nitrite .	49
Table 4.7 Sample analysis and recovery percentage of spiked samples determined by the paper-based platform.....	52
Table 4.8 Comparison of the performance of different analytical platforms for nitrite detection using the Griess reaction	54
Table 5.1 The optimum conditions using the thread-based device	59
Table 5.2 The optimum conditions using the paper-based device.....	59

LIST OF FIGURES

	Page
Figure 2.1 Diazotization reaction	5
Figure 2.2 Structure of sulfanilic acid.....	5
Figure 2.3 Structure of 1-naphthylamine.	6
Figure 2.4 The reaction of nitrite with common Griess assay.....	6
Figure 2.5 Paper-based device (a) for nitrate detection (b) for nitrite detection (DZ: detection zone, TC: transport channel, RC: reduction channel, IS: interleaving sheet)	8
Figure 2.6 Paper-based device for nitrite and pH sensing (reprinted with permission from.....	9
Figure 2.7 Structure of chromotropic acid.....	10
Figure 3.1 Scheme of the thread surface modification.....	15
Figure 3.2 Scheme of the paper surface modification.....	17
Figure 3.3 The paper-based platform.....	18
Figure 3.4 Steps in nitrite detection by the paper-based platform; (A) a piece of circular modified paper after nitrite extraction was placed on the detection zone of the paper-based platform, (B) Deionized water was dropped on the platform folded in half to dissolve CTA, and (C) The dye was formed onto the modified paper.....	19
Figure 4.1 IR spectra of unwaxed cellulose thread and the modified thread after nitrite detection.....	21
Figure 4.2 Raman spectra of the thread materials.....	22
Figure 4.3 The expected product on the surface of the materials after nitrite detection.....	23

Figure 4.4 Effect of chromotropic concentration in (A) 0.05 M, (B) 0.10 M, and (C) 0.20 M sulfuric acid on the dye band length observed in the detection of nitrite.	26
Figure 4.5 Effect of sample volume on nitrite detection using (A) 5 mM and (B) 10 mM chromotropic acid in 0.1 M sulfuric acid.	28
Figure 4.6 Effect of 0.2 M citric acid addition to 5 mM chromotropic acid in 0.1 M sulfuric acid on nitrite detection.	30
Figure 4.7 Calibration curve for nitrite determination by thread-based platform using reagent solution containing 0.2 M citric acid and 5 mM chromotropic acid in 0.10 M sulfuric acid with 5-time sample introduction (15 μ L).	32
Figure 4.8 The photographs of the thread platform.	32
Figure 4.9 Raman spectra of the paper materials.	37
Figure 4.10 Effect of <i>p</i> -nitrobenzoyl chloride (PNB) amount used in the paper surface modification in the detection of nitrite (inset – photographs of the papers).	40
Figure 4.11 Effect of citric acid (CA) concentration in the detection of nitrite ion (A) photograph of testing papers and (B) the effect of citric acid concentration on the observed gray intensities (inset – effect on the detection at low nitrite concentrations).	42
Figure 4.12 Effect of sample volume in the detection of nitrite ion (A) photograph of testing papers and (B) the effect of sample volume on the observed gray intensities (inset – effect on the detection at low nitrite concentrations).	44
Figure 4.13 Effect of extraction time in the detection of nitrite ion (A) photograph of testing papers and (B) the effect of extraction time on the observed gray intensities (inset – effect on the detection at low nitrite concentrations).	46
Figure 4.14 Effect of chromotropic acid (CTA) amount used in the reagent zone of the paper-based platform in the detection of nitrite (inset – photographs of the papers).	48

Figure 4.15 Calibration curve for nitrite determination by paper-based platform using 3-mL sample volume in 0.20 M citric acid and 100 μ M chromotropic acid in the reagent zone with 15-minute extraction time..... 50



CHAPTER I

INTRODUCTION

1.1 Statement of the problem

Nitrite is widely found in the environment, agricultural runoffs from the denitrification and nitrification processes in soil containing nitrogenous fertilizers [1], the wastewater streams from dye manufacturing [2], and a preservative in food products [3]. In food products, nitrite is used as food additives to inhibit the growth of *Clostridium botulinum* in processed meat [3]. Nitrite is also rich in leafy vegetables and fruits [4]. Due to the health concern, nitrite ion was the subject of interest in this research. Nitrite ion, even at trace level, could potentially be hazardous to human health as it causes methemoglobinemia affecting the oxygen transport system [5-7] mainly in children and women during pregnancy [8-10]. Moreover, a lot of research on the toxicity reported that nitrite could react with secondary amines and amides to generate carcinogenic *N*-nitroso compounds [11, 12] and might increase the risk of gastrointestinal cancer [13, 14]. Therefore, there are regulations for the maximum permitted use levels for nitrite legislated in many countries.

Various analytical techniques were served to determine the level of nitrite including ion chromatography, capillary electrophoresis, and electrochemical techniques [15-18]. However, these techniques are prone to be a tedious and time-consuming process and need high-skilled operators to operate them; moreover, the cost of instrumentation is high. Methods, therefore, that enable on-site detection of

nitrite are highly desirable. In this research, the Griess assay was adopted to determine the level of nitrite [19]. This assay produces an azo dye whose color intensity is proportional to nitrite concentration. Two platforms based on Griess assay were developed for the determination of nitrite. The first platform is a thread-based device, while the other is a paper-based device. These colorimetric detection methods can be alternatives to instrumental analysis with the possibility for on-site analysis.

1.2 Objective of the research

The objective of this research was firstly to establish the platforms for the colorimetric determination of nitrite ions, and afterward, to apply these platforms to determine nitrite ions in various kinds of real samples.

1.3 Scope of the research

The scope of this research includes the establishment and the application of the platforms for the determination of nitrite ions in various kinds of real samples. Parameters affecting the determination including reagent concentrations, reaction time, and sample volume were investigated.

CHAPTER II

THEORY AND LITERATURE REVIEW

2.1 Nitrite

Nitrite is widely used throughout chemical [2], food [3], pharmaceutical industries [20]. In the environment, nitrite is a general intermediate in the nitrogen cycle [21]. It is also found in green leafy vegetables [4, 22] such as cabbage, carrot, beetroot, etc. Although, nitrite does not naturally occur in mineral form, it is basically produced as an intermediate compound of denitrification and nitrification processes from the organic nitrogen-containing substances carried out by microorganisms [1]. Subsequently, small amounts of nitrite could pass through the soil and potentially contaminate the ground water. To increase plant production, the nitrogenous fertilizers were extensively applied in modern farming. Contamination of residual nitrogen-containing fertilizer in soil would elevate the level of nitrite in ground water as well as in surface waters.

The major use of nitrite is a food additive in processed meats, fish, and cheeses. There are three main functions of the nitrite addition in food. It enhances the flavor and acts as a color stabilizer [15, 23, 24]. It also inhibits the growth of *Clostridium botulinum* [3], which is one of food spoilage bacteria.

As mentioned above, nitrite has many advantages. It, however, causes danger to human health. The intake of high levels of nitrite can cause methemoglobinemia or

blue baby syndrome [8-10] that affects the impaired oxygen delivery to tissues [5-7]. Apart from the acute toxicity, nitrite could react with secondary amines and amides in the stomach to generate *N*-nitroso compounds [12] which have been reported to be carcinogenic in at least 40 animal species [11, 25-27]. Moreover, the consumption of nitrite from drinking water and other dietary sources can increase the risk of gastrointestinal cancer in humans [13, 14] hence the authorization in every country has regulations related in this crisis. In the same way in Thailand, the maximum permitted level for nitrite in drinking water, tap water, and food was established as shown in Table 2.1.

Table 2.1 The maximum permitted levels for nitrite in drinking water, tap water, and food in Thailand [28-30]

Sources	Maximum permitted level
Drinking water	3 mg/L (65 μ M)
Tap water	3 mg/L (65 μ M)
Food	125 mg/kg ^a

^acalculated as sodium nitrite

Due to these toxic effects, innumerable methods have been developed for the detection and the determination of nitrite [15-18]. This research is focused on the analysis of nitrite in various samples using the Griess reagent.

2.2 Diazotization reaction and Griess reaction

Diazotization is one of the derivatization pathways that converts the primary aromatic amines to diazonium ion or diazonium salt after the reaction with nitrite in an acidic condition [31]. The reaction is shown as followed.

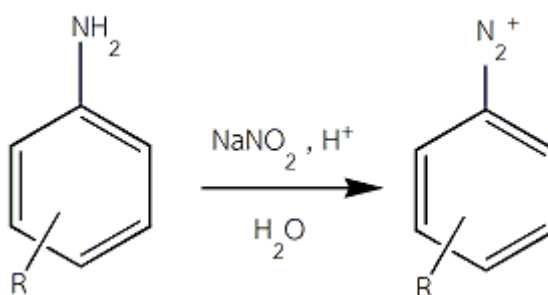


Figure 2.1 Diazotization reaction [31].

Diazonium salts are dominant synthetic intermediates that further undergo the coupling reaction with aromatic compounds to produce azo dyes. The obtained dye can be determined by naked-eye or a spectroscopic technique.

The Griess reaction [19] is the assay that has been used to determine nitrite ions. The Griess assay was initially proposed in 1879 [32] and it remains popular. It consists of two subsequent steps: diazotization and coupling reactions. Nitrite ions in sulfuric acid firstly react with sulfanilic acid (Figure 2.2) to form diazonium ions that subsequently react with 1-naphthylamine (Figure 2.3) to produce water-soluble azo dyes. This composition was later called Griess reagent.

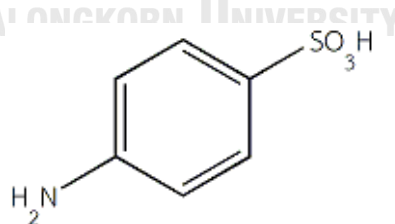


Figure 2.2 Structure of sulfanilic acid.

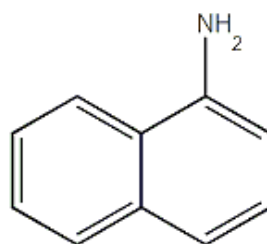


Figure 2.3 Structure of 1-naphthylamine.

Instead of the classical Griess reagent, numerous sulfanilic acid derivatives were used as the primary aromatic amines and the most popular derivative is sulfanilamide. Moreover, *N*-(1-naphthyl)ethylenediamine (NED) [33] replaced 1-naphthylamine in this reaction because the latter is a carcinogenic reagent. The most common and commercial Griess reagents, therefore, are sulfanilamide and NED. The reaction of these reagent mixture with nitrite occurs as shown in Figure 2.4.

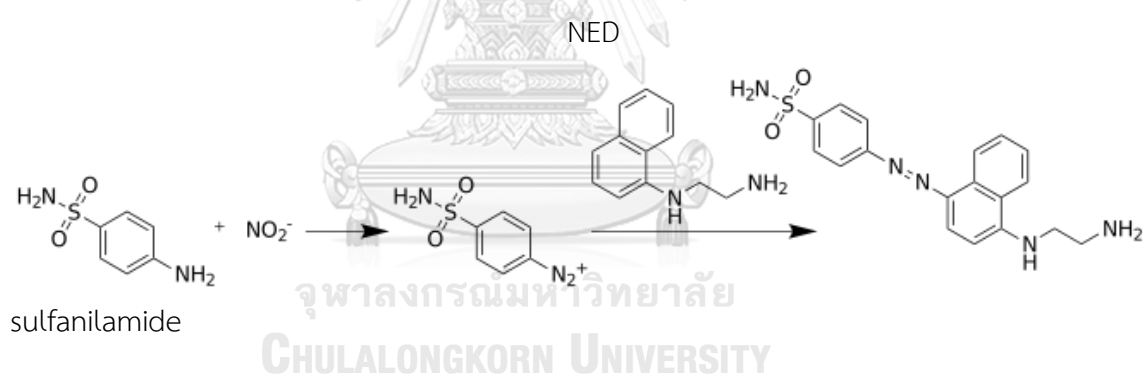


Figure 2.4 The reaction of nitrite with common Griess assay.

The Griess reagent was successfully applied to determine nitrite in many studies due to its specificity and ease of use. In this work, the diazotization and coupling reaction as occurred in Griess assay were adopted to determine the concentration of nitrite. However, sulfanilamide was very sensitive to light. Some researchers claimed that aniline-like compounds could be readily oxidized in air [34], while NED that was used to replace carcinogenic 1-naphthylamine is also carcinogenic [35]. Therefore, alternative Griess reagents were used in this work and described in the next section.

2.3 Thread-based and paper-based devices for the determination of nitrite

Conventional instrumental techniques to determine the concentration of nitrite including ion chromatography often involve tedious and time-consuming processes. Moreover, it requires highly skilled personnel to operate. Therefore, colorimetric methods have been developed to overcome the detection difficulties with a requirement of a simple instrument (*i.e.* UV/Vis spectroscopy) or simple platforms such as paper and thread. Thread-based analytical devices (TADs) and paper-based analytical devices (PADs) are gaining considerable ground due to the simplicity, cost effectiveness, and rapid analysis. These TADs and PADs have also been used as platforms for the determination of nitrite based on Griess reaction.

Jayawardane *et al.* [36] developed a microfluidic PAD for the determination of nitrite and nitrate using Griess reaction (*i.e.* sulfanilamide and NED acidified by citric acid). The μ -PAD is shown in Figure 2.5. For nitrate detection, it was firstly reduced to nitrite by zinc microparticles deposited on the device reaction zone and consecutively reacted with the Griess reagent. The color intensity (the intensity of the green color) was determined. This device was successfully applied to determine nitrite and nitrate in water samples. The obtained limit of detection (LOD) and limit of quantification (LOQ) were 1.0 and 7.8 μM with a 20- μL of sample volume, respectively, while LOD and LOQ for nitrate determination were 19 and 48 μM with the same size of volume in nitrite detection, respectively. The working range of this method was up to 50 and 200 μM for nitrite and nitrate, respectively.

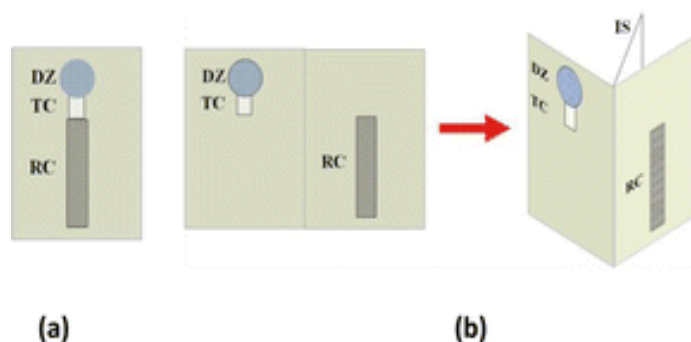


Figure 2.5 Paper-based device (a) for nitrate detection (b) for nitrite detection (DZ: detection zone, TC: transport channel, RC: reduction channel, IS: interleaving sheet) (adapted with permission from [36]).

Bhakta *et al.* [37] also used Griess reagent (*i.e.* sulfanilamide and NED acidified by phosphoric acid) on a paper-based platform to detect nitrite in saliva. The LOD of this method was 10 μM with a 12- μL of sample volume. In addition, Lopez-Ruiz *et al.* [38] developed a paper-based platform to simultaneously determine the concentration of nitrite and the pH values in drinking water. The device consisted of a zone for sample introduction in the middle connected to seven sensing areas containing different immobilized reagents by independent channels, and one blank zone (reference area) located separately on the same device (Figure 2.6). Two different pH indicators (phenol red and chlorophenol red) were used to modify the pH sensing areas (1 to 4). The other areas were the nitrite sensing areas (5 to 7) modified with Griess reagents (*i.e.* sulfanilamide and NED acidified by citric acid). The LOD of this method was 0.52 mg/L nitrite with a 30- μL of sample volume.

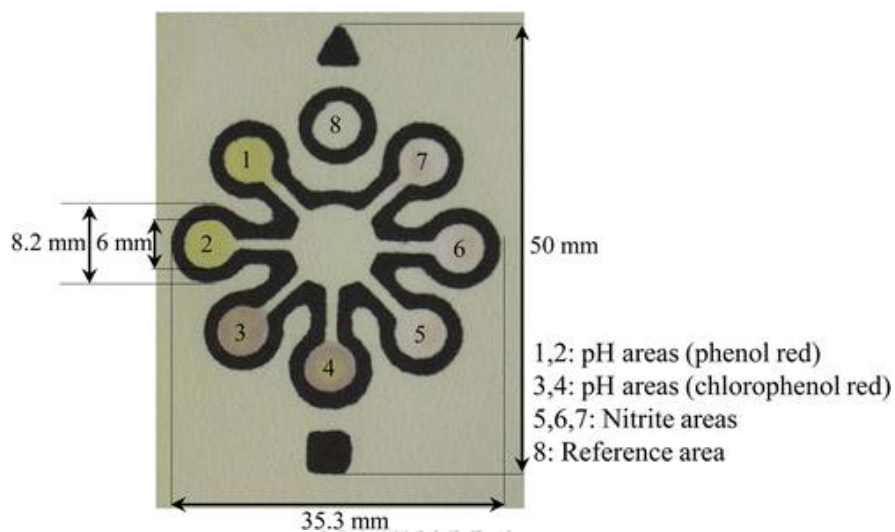


Figure 2.6 Paper-based device for nitrite and pH sensing (reprinted with permission from [38]).

As previously described, most paper-based devices had the same drawback which is the limited volume of introduced sample. This could limit the sensitivity of the detection of nitrite at low concentration level. To improve the sensitivity of method, increasing sample size is one of alternatives. A chemically modified cellulose paper was prepared for extraction of nitrite in this work. It could be used with a large sample volume to detect nitrite at low concentration. In this research, sulfanilamide was replaced by *p*-aminobenzoyl functional group chemically modified on the material surface as it is more stable to light exposure. Nontoxic chromotropic acid or CTA (Figure 2.7) replacing NED was used as a coupling reagent.

The process of nitrite determination by our paper-based platform started from the extraction of nitrite in solution by the modified paper. After diazonium ions were generated on the surface, the coupling reaction was consecutively performed. With this fashion of determination, the sample volume could be increased, and trace nitrites could be detected. Aside from that, it is to be emphasized that the step of extraction would separate nitrite ions from the other interfering species in the sample. Hence,

these species could not potentially interfere the relevant reactions. Based on this assumption, detection limit of the method should be improved.

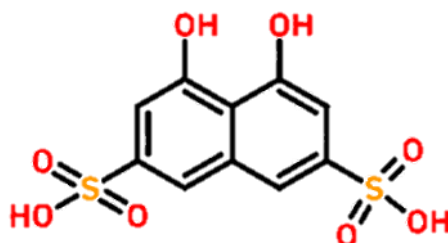


Figure 2.7 Structure of chromotropic acid.

For thread-based analytical devices, Nilghaz *et al.* [39] developed thread-based analytical devices. This device was based on the colorimetric reaction and length-based detection. Some part of their study was focused on nitrite detection based on Griess assay (*i.e.* sulfanilamide acidified by citric acid and NED). The azo dye was generated and absorbed on the thread while nitrite diffused along the length of the thread. The color band length was proportional to the nitrite concentration and measured by a ruler. The linear range was from 0 - 1,000 μM .

From above mentioned research, the Griess reagents were dropped onto the platform before use. The introduction of several reagents onto the platform is prone to the unequal distribution of the reagents along the thread. It is also required that the diazotization/coupling reaction and the dye absorption on the thread surface should occur quickly. This also limits the sample volume used on the platform as large volume of sample would elute the reagents to the boarder of the detection area. To eliminate these drawbacks, a thread-based platform in this work was chemically modified with *p*-aminobenzoyl moiety followed by impregnation of CTA. In the presence of nitrite, diazonium ions occurred directly on the thread surface. Therefore, it would eliminate the effect of reagent diffusion or dye absorption. Moreover, the

method could increase the uptake of solution volume without elution of the dye products. According to these assumptions, the thread platform should be able to detect low level of nitrite, while the unequal distribution of the reagent would also be minimized.



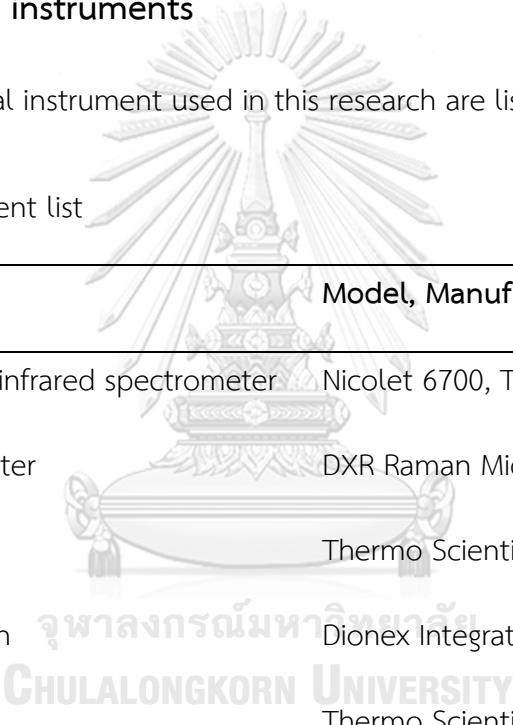
CHAPTER III

EXPERIMENTAL

3.1 Analytical instruments

All analytical instrument used in this research are listed in Table 3.1.

Table 3.1 Instrument list



Instruments	Model, Manufacture
Fourier-transform infrared spectrometer	Nicolet 6700, Thermo Scientific
Raman spectrometer	DXR Raman Microscope, Thermo Scientific
Ion chromatograph	Dionex Integration RFIC system, Thermo Scientific

3.2 Chemicals

The reagents and solvents used in this research are listed in Table 3.2. All chemicals are of analytical grade and used without further purification.

Table 3.2 Chemicals list

Chemicals	Supplier
Sodium nitrite	Merck
Chromotropic acid	Merck
<i>p</i> -nitrobenzoyl chloride	Merck
Sodium dithionite	Merck
Citric acid	Merck
Sodium chloride	Merck
Sodium bicarbonate	Merck
Sodium nitrate	Merck
Potassium chloride	Merck
Potassium nitrate	Merck
Ammonium acetate	Merck
Ammonium nitrate	VWR Chemicals BDH
Iron (II) nitrite	Merck
Sodium hydroxide	Merck

Table 3.2 Chemicals list (*Cont.*)

Chemicals	Supplier
Sodium dihydrogenphosphate	Merck
Calcium nitrate	UNIVAR
Magnesium nitrate	UNIVAR
Sulfuric acid (95-97% w/w)	Merck
Acetronitrile	Merck

3.3 Determination of nitrite by thread-based platform

3.3.1 Synthesis of modified cellulose thread and characterization

The natural wax of the cotton yarn was removed to improve the hydrophilicity and facilitate liquid wicking of cotton thread. The natural cotton yarn (120 cm) was immersed in a 1 M sodium hydroxide solution (50 mL) and heated at 60°C for 3 hours. The cotton yarn was then washed with deionized water until the pH of runoff was neutral and dried under ambient condition. The unwaxed thread had diameter *ca.* 1.34±0.06 mm measured by a micrometer from 30 random samples. The unwaxed thread (100 cm) was put in 40 mL of acetonitrile containing 0.01 mole *p*-nitrobenzoyl chloride and heated at 60°C for 4 hours. To eliminate unattached reagent, the yarn was washed with deionized water until the color of the yarn turned from yellow to off-white. Finally, the yarn was further suspended in 50 mL of 0.2 M sodium dithionite solution and heated at 50°C for 24 hours. The final material was washed with deionized

water and dried under ambient condition. The material color was white. The synthesis scheme is present in Figure 3.1.

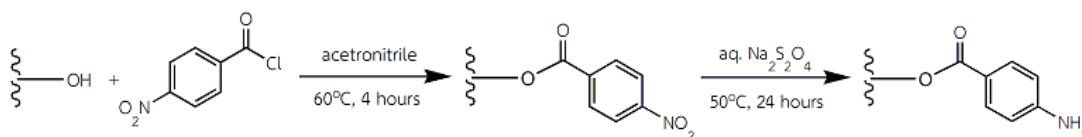


Figure 3.1 Scheme of the thread surface modification.

After each modification step, the obtained materials were tested with ninhydrin assay and characterized by FT-IR in ATR mode and Raman spectroscopy. Each modified yarn composed of nine thread with 0.36 ± 0.04 mm in diameter measured by a micrometer from 30 random samples. The thread was used to determine the concentration of nitrite.

3.3.2 Determination of nitrite by the thread platform

Chromotropic acid (CTA) of appropriate amount was dissolved in sulfuric acid solution (90 mL) and dropped onto a piece of 6-cm modified cellulose yarn. The yarn was untwisted into 9 individual threads after it was dried for 30 minutes. A knot was tied in the middle of the thread to serve as a standard or sample introduction zone. The thread was further fixed between polyacrylic sheets and used as the platform for nitrite detection.

To detect nitrite, a standard or sample solution ($3 \mu\text{L}$) was dropped onto the knot in the middle of the thread. The introduced solution diffused throughout the length of the thread starting from the knot. A 3-minute interval time between each sample introduction was applied to repeat the solution introduction. In our preliminary study, a volume of $3 \mu\text{L}$ was enough for the solution to diffuse along the thread. After

introducing a solution containing nitrite onto the thread platform, an azo dye was formed along the length of the thread observed as a pink colored band. Photographs of the threads were taken in a studio box 20 minutes after the last sample injection and the length of the color band was measured. The effect of sulfuric acid concentration, CTA concentration, sample volume, and interferences were investigated.

3.3.3 Real samples analysis

The sample preparation was adapted from the GB 5009.33-2016 method (determination of nitrite and nitrate in food) [40]. Sample (*i.e.* sausage, Chinese cabbage) was firstly ground in a blender. Ten grams of ground sample was extracted by 30 mL of deionized water. Then, a 2.6% w/v borax solution (1.2 mL) was added in the mixture, and further heated to 70°C while stirring for 15 minutes. The mixture was cooled on an ice bath for 15 minutes. The extracting solution was filtered and transferred to another container. A 15% w/v of potassium ferricyanide solution (0.5 mL) was added. After shaking, a 30% w/v zinc acetate solution (0.5 mL) was added to precipitate the protein. The solution was filtered again through a 0.1- μ m syringe filter to remove residuals. The obtained solution was subjected to the nitrite analysis by the thread platform. In case of Chinese cabbage sample preparation, the potassium ferricyanide and zinc acetate solutions were not used. In case of drinking water sample preparation, the samples were filtered through 0.1- μ m syringe filters prior to the test.

3.4 Determination of nitrite by paper-based platform

3.4.1 Synthesis of modified cellulose paper and characterization

A piece of Thomas Baker No.1 qualitative filter paper (125 mm i.d.) was suspended in a solution containing an appropriate amount of *p*-nitrobenzoyl chloride in acetonitrile (100 mL) and heated at 80°C for 4 hours. The obtained paper was washed by deionized water to eliminate unattached reagent until the color of the paper turned from yellow to off-white. The obtained paper was further suspended in 100 mL of 0.2 M sodium dithionite solution and heated at 50°C for 24 hours. The resulting paper was washed by deionized water and dried under ambient condition. The final product color was white. The synthesis scheme is present in Figure 3.2.

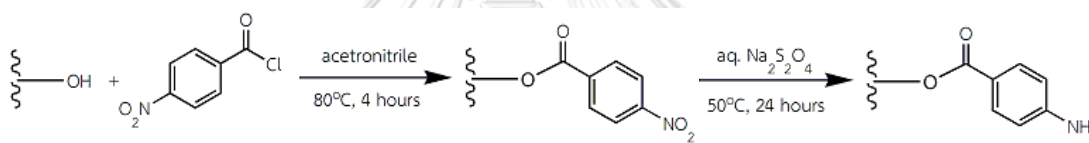


Figure 3.2 Scheme of the paper surface modification.

After each modification process, the obtained papers were tested by ninhydrin assay and characterized by Raman spectroscopy.

3.4.2 Determination of nitrite by the paper platform

A design of paper-based platform is shown in Figure 3.3. A Whatman No.1 filter paper was used as platform for screen printing which was consisted of 2 parts. The first part was a detection zone where the modified paper was placed after the nitrite extraction. The other part was the reagent zone containing CTA of appropriate amount. A CTA solution was dropped on the reagent zone and dried before use. These two

zones were designed in the same vertical position when the platform was folded in half to overlay the reagent zone on top of the detection zone.

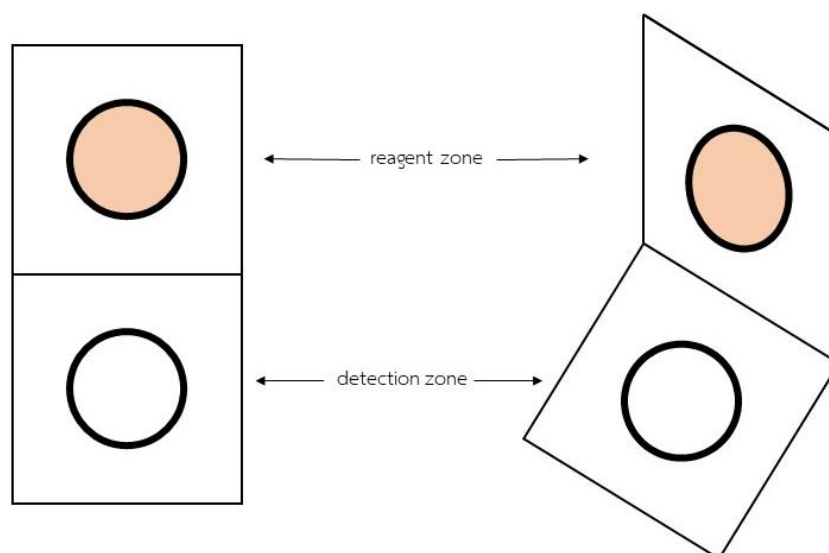


Figure 3.3 The paper-based platform.

To prepare a paper sensor, a piece of modified paper was cut into pieces of circular shape (*ca.* 5.2 mm i.d.). Each paper was immersed in an acidified nitrite standard or sample solution and stirred in ambient condition for a specific time for diazotization reaction to occur on the paper surface. After stirring, the paper was further placed on the detection zone of the paper-based platform. The platform was then folded in half to cover the detection zone with the CTA reagent zone. 3 μL of deionized water was dropped on top of the reagent zone to dissolve the attached CTA. The dissolved CTA was injected directly onto the surface of the modified paper on the detection zone to complete the coupling reaction with the diazonium ions on the paper surface. The dye of pink color was formed on the paper surface (Figure 3.4). The modified paper was then removed from the platform, dipped in deionized water to remove excess reagent, and let dried at room temperature (*ca.* 10 min). Photographs of the dried papers were taken in a controlled light studio box and were processed by

ImageJ software. The intensity of gray value was collected. The effect of *p*-nitrobenzoyl chloride amount, citric acid concentration, sample volume, extraction time, CTA concentration, and interferences were investigated.

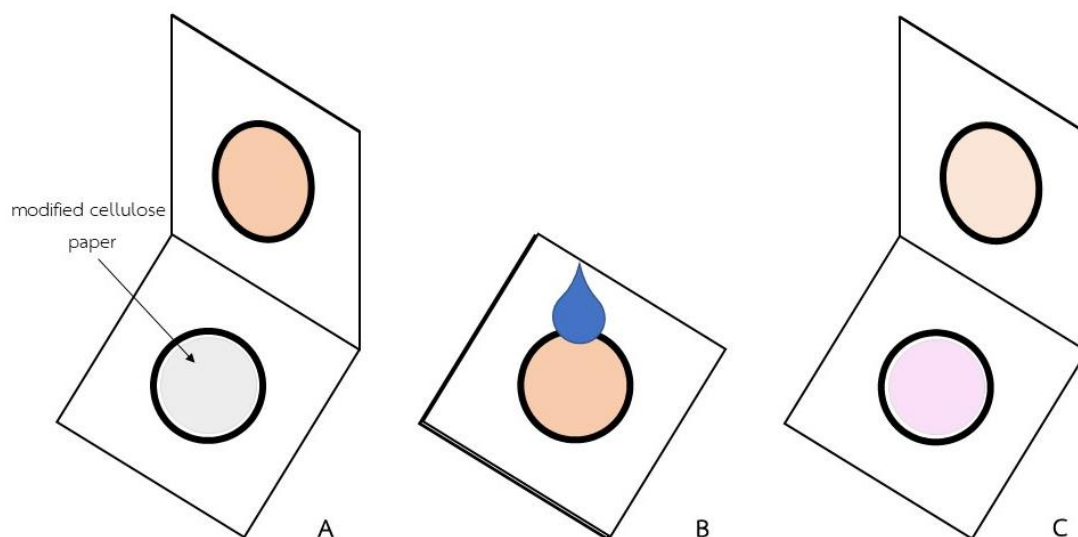


Figure 3.4 Steps in nitrite detection by the paper-based platform; (A) a piece of circular modified paper after nitrite extraction was placed on the detection zone of the paper-based platform, (B) Deionized water was dropped on the platform folded in half to dissolve CTA, and (C) The dye was formed onto the modified paper.

จุฬาลงกรณ์มหาวิทยาลัย
CHULALONGKORN UNIVERSITY

3.4.3 Real samples analysis

Agricultural runoff from a botanic greenhouse, paddy fields, and a Chinese kale garden were collected. Large particles were removed from all samples by filtration. The obtained samples were subsequently filtered through 0.1- μm syringe filters prior to the test.

CHAPTER IV

RESULTS AND DISCUSSION

4.1 Determination of nitrite by thread-based platform

4.1.1 Characterization

To prepare the thread platform, the surface of cellulose thread was modified in two steps (Figure 3.1). In the first step, the hydroxyl groups on cellulose was substituted by *p*-nitrobenzoyl chloride resulting in *p*-nitrobenzoyl-thread. In the second step, the reduction of *p*-nitrobenzoyl moiety was done yielding *p*-aminobenzoyl-thread. The obtained materials were further characterized.

The ninhydrin test was performed on unwaxed cellulose thread and *p*-aminobenzoyl-thread to observe primary amine groups. The results showed a positive test result on *p*-aminobenzoyl-thread as the thread turned purple, while unwaxed cellulose thread color remained off-white. This result confirmed the presence of primary amine group on the modified thread, resulted from the surface modification with *p*-aminobenzoyl moiety.

ATR-FTIR was performed to characterize the unwaxed cellulose thread, *p*-nitrobenzoyl-thread, *p*-aminobenzoyl-thread, and the modified thread after nitrite detection (Figure 4.1). The results show that only the characteristic bands of cellulose [41] ($2,980\text{ cm}^{-1}$ C-H stretching and $3,320\text{ cm}^{-1}$ O-H stretching of hydroxyl group) were observed in the spectra of all samples. However, the characteristic signal for the C=O

stretch ($1,600 - 1,850 \text{ cm}^{-1}$) was not found in either the spectra of the *p*-nitrobenzoyl-thread or the *p*-aminobenzoyl-thread. The possible explanation might be that there was a low content of *p*-nitrobenzoyl or *p*-aminobenzoyl moieties attached on the cellulose.

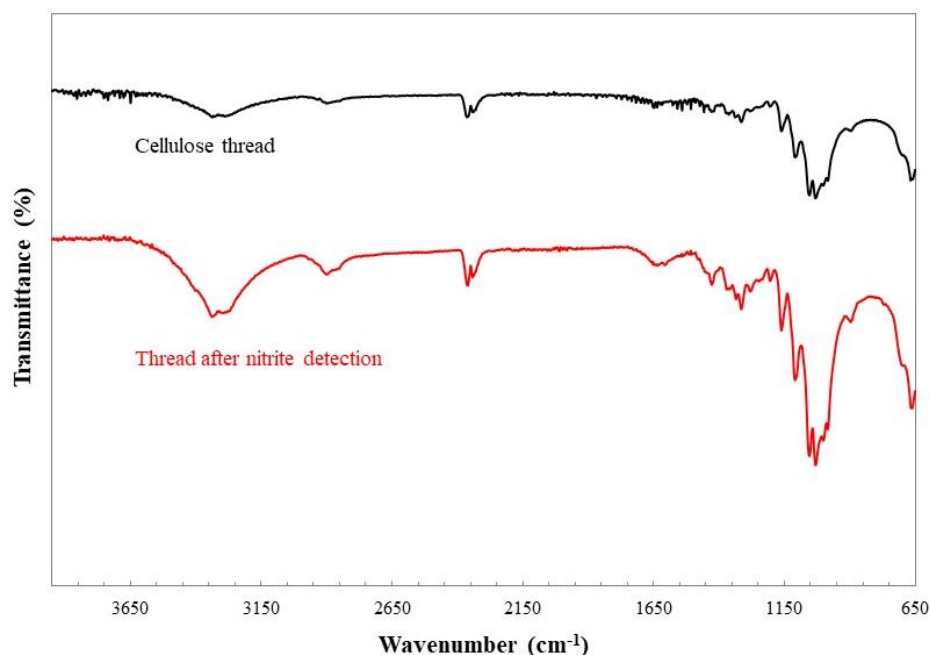


Figure 4.1 IR spectra of unwaxed cellulose thread and the modified thread after nitrite detection.

The threads were further characterized by Raman spectroscopy as shown in Figure 4.2 and Table 4.1. The signal in the Raman spectrum of the unwaxed cellulose thread exhibited two peaks at $1,093 \text{ cm}^{-1}$ and $1,120 \text{ cm}^{-1}$ attributed to the C-O stretching of glycosidic link or C-OH in cellulose. These peaks were also present in every samples. The additional peaks at $1,290 \text{ cm}^{-1}$ and $1,336 \text{ cm}^{-1}$ was observed in the Raman spectrum of the *p*-nitrobenzoyl cellulose thread which could be assigned to C-O-C stretching of para-substituted benzoate in symmetric mode and asymmetric mode, respectively. In addition, the presence of a signal of symmetric C-NO₂ stretching of aromatic nitro compound at $1,377 \text{ cm}^{-1}$ confirmed that the *p*-nitrobenzoyl moiety

was successfully attached to the cellulose skeleton. After the reduction reaction, the signal of N-H deformation of primary amino group additionally appeared at $1,602\text{ cm}^{-1}$, revealing that the reduction of the nitro group to amino group was successfully done. Nevertheless, the signal of symmetric C-NO₂ stretching of aromatic nitro compound was still present in the Raman spectrum of the *p*-aminobenzoyl-thread. It indicated that the reduction of all the nitro groups on the thread was not completely done.

The expected functional group on the thread surface after diazotization and coupling reaction is shown in Figure 4.3. The spectrum of the modified thread after nitrite detection exhibited the signals of the N=N stretching of the azo bond at $1,409\text{ cm}^{-1}$ and $1,510\text{ cm}^{-1}$. Moreover, the signal of the C-N stretching of the carbon adjacent to the azo bond at $1,290\text{ cm}^{-1}$ became stronger and broader until it overwhelmed the signal at $1,336\text{ cm}^{-1}$. These results confirmed that the diazotization occurred on the modified thread surface.

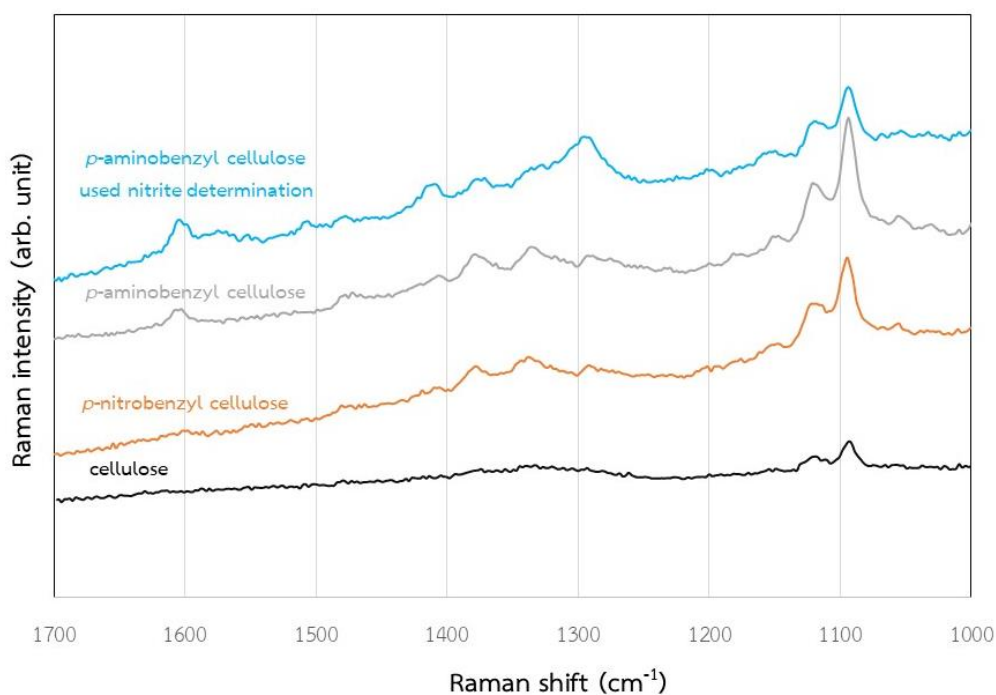


Figure 4.2 Raman spectra of the thread materials.

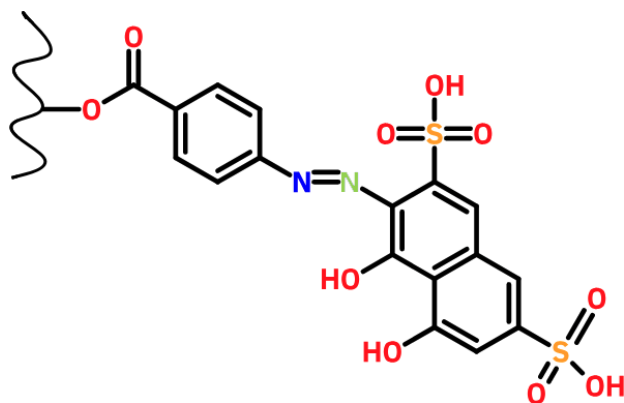


Figure 4.3 The expected product on the surface of the materials after nitrite detection.



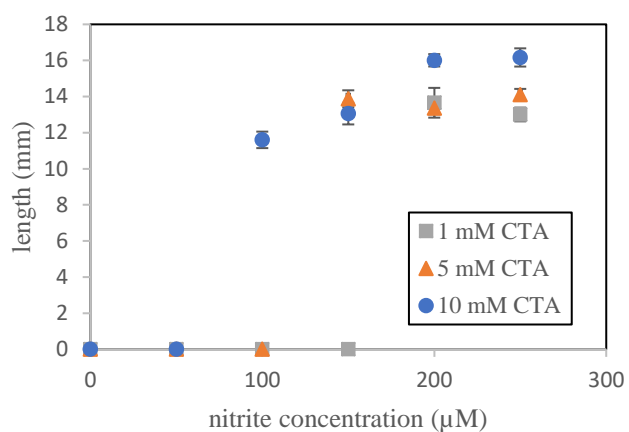
Table 4.1 Wavenumber and Raman band assignments for thread materials [41]

Material	Functional Groups	Wavenumber (cm ⁻¹)
Unwaxed cellulose thread	C-O stretching of C-O-C (glycosidic link) or C-OH in cellulose	1,093
	C-O stretching of C-O-C (glycosidic link) or C-OH in cellulose	1,120
Additional Functional groups		
<i>p</i> -nitrobenzoyl thread	C-O-C stretching of para-substituted benzoate (symmetric)	1,290
	C-O-C stretching of para-substituted benzoate (asymmetric)	1,336
	C-NO ₂ stretching of aromatic nitro compound (symmetric)	1,377
<i>p</i> -aminobenzoyl thread	C-O-C stretching of para-substituted benzoate (symmetric)	1,290
	C-O-C stretching of para-substituted benzoate (asymmetric)	1,336
	C-NO ₂ stretching of aromatic nitro compound (symmetric)	1,377
	N-H deformation of primary amino group	1,602
Modified thread after nitrite detection	C-N stretching of carbon adjacent to the azo bond	1,290
	C-NO ₂ stretching of aromatic nitro compound (symmetric)	1,377
	N=N stretching of azo bond	1,409
	N=N stretching of azo bond	1,510
	N-H deformation of primary amino group	1,602

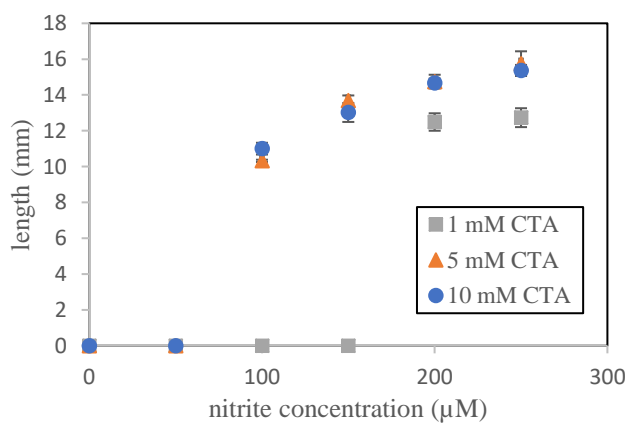
4.1.2 Effect of chromotropic acid and sulfuric acid concentration

The effect of chromotropic acid (CTA) and sulfuric acid concentration were simultaneously investigated to find the condition yielding a high detection sensitivity. A standard nitrite solution (3 μL) was introduced on the thread platform three times with a 3-minute time interval between each solution introduction. Sulfuric acid with concentration of 0.05, 0.10, and 0.20 M were used, while the chromotropic acid concentration was varied from 1.0 to 10.0 mM. The experiments were done in triplicate and the results are shown in Figure 4.4.

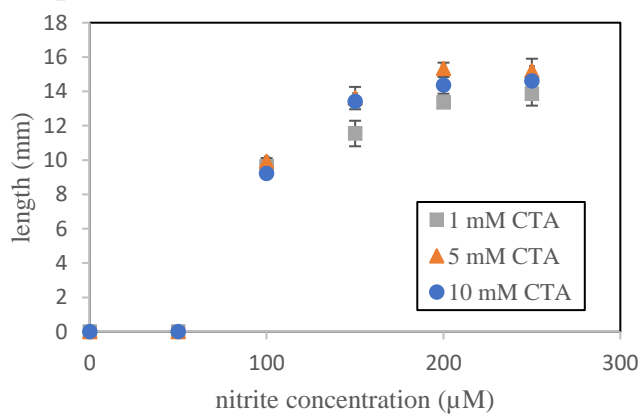




(A)



(B)



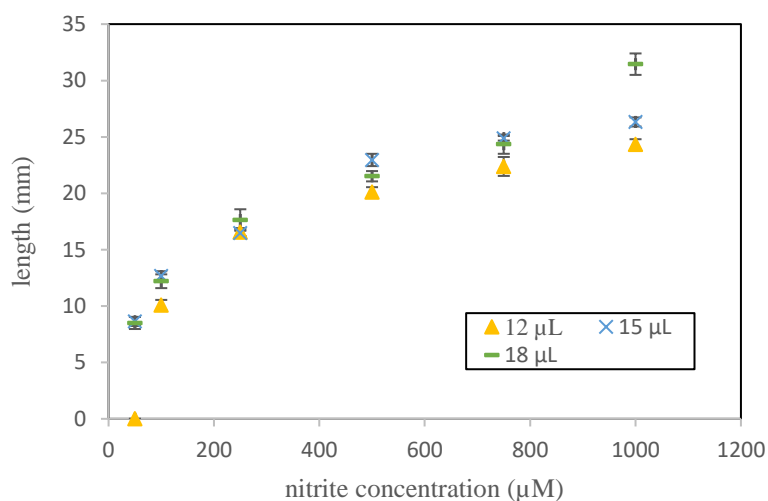
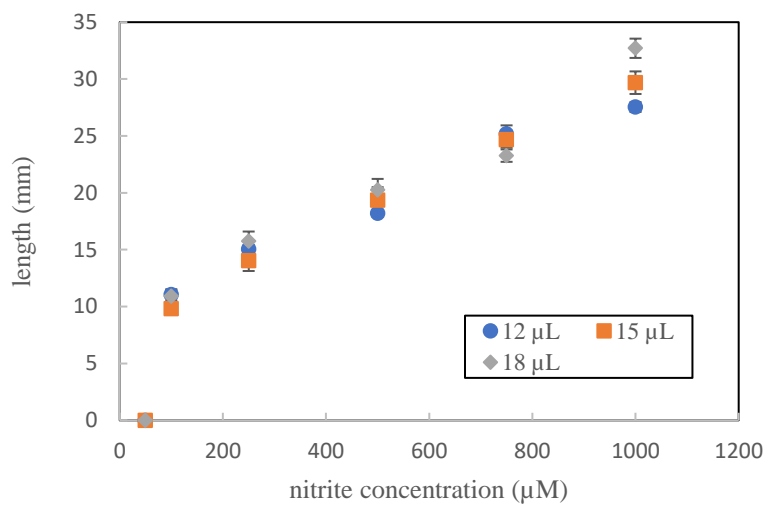
(C)

Figure 4.4 Effect of chromotopic concentration in (A) 0.05 M, (B) 0.10 M, and (C) 0.20 M sulfuric acid on the dye band length observed in the detection of nitrite.

According to the results in Figure 4.4 (A), owing to weak intensity of the band color on the thread, nitrite at low levels could not be detected when 0.05 M sulfuric acid was used. The detection of 100 μM nitrite was possible when the concentration of sulfuric acid was increased to 0.10 M and 0.20 M with various concentrations of chromotropic acid (Figure 4.4 (B) and (C)). However, the use of 1 mM chromotropic acid produced pale color on the thread which was difficult to visualize. The concentration of sulfuric acid clearly had a strong effect on the diazotization reaction, and it should be high enough for the reaction to occur. Nevertheless, the color band length did not significantly increase in the detection of a very high concentration of nitrite (200 or 250 μM) despite the use of high concentration of both sulfuric acid and chromotropic acid. It is probable that a large amount of nitrous acid was produced at a high concentration of nitrite when the sample was in contact with acid on the thread surface. A specific amount of nitrous acid may turn to NO and NO₂ gas and released from the thread surface before diazotization could occur [42]. The chromotropic concentration of 5 and 10 mM in 0.10 M sulfuric acid were selected for further investigation.

4.1.3 Effect of sample volume

The sample volume is one of parameters to be optimized to improve the sensitivity of the method. In the previous experiment, the thread used to detect low level nitrite did not show detectable color band with a sample volume of 9 μL (3 μL \times 3 times). In an attempt to detect nitrite at low concentration level, a higher sample volume (12 and 18 μL) was applied with the same procedure as described in session 3.3.2. The experiments were done in triplicate and the results are shown in Figure 4.5.



(B)

Figure 4.5 Effect of sample volume on nitrite detection using (A) 5 mM and (B) 10 mM chromotropic acid in 0.1 M sulfuric acid.

A wider nitrite concentration range (100-1000 μM) could be detected in increasing the sample volume. However, there was not a significant change in color band length when the sample volume was increased to 18 μL , possibly due to the limit of liquid capacity of the thread. In addition, the use of 5 mM CTA in 0.10 M sulfuric

acid provided a relatively linear relationship between the band length and nitrite concentration compared to 10 mM CTA. Although, the use of 10 mM CTA in 0.10 M sulfuric acid with the sample volume of 15 and 18 μL could produce an observable color band for 50 μM nitrite detection, a linear relationship was not obtained. Therefore, the sample volume of 12 and 15 μL and reagent solution containing 5 mM CTA in 0.10 M sulfuric acid was chosen for further study.

4.1.4 Effect of citric acid addition

According to preliminary results, alkaline species in samples strongly affected the color development due to the lowering of the acidity on the platform. Consequently, the diazotization reaction could not occur properly. In this research, the effect of alkaline species existing in the real samples would be suppressed by adding citric acid. A reagent solution containing CTA in sulfuric acid and 0.2 M citric acid was used to modify the thread platform. The results are shown in Figure 4.6. Surprisingly, the color on thread was more intense in the presence of citric acid and the detection of 50 μM nitrite could be achieved. Moreover, the band length dramatically increased in increasing the nitrite concentration from 50 to 100 μM , while the band length gradually increased at higher concentration of nitrite. It could be explained by the limited amount of chromotropic acid on the thread. A better sensitivity and linear relationship were achieved by using a sample volume of 15 μL . Therefore, using a sample volume of 15 μL (3 μL \times 5 times) was adopted in the nitrite detection on the thread platform modified with the reagent containing 0.2 M citric acid.

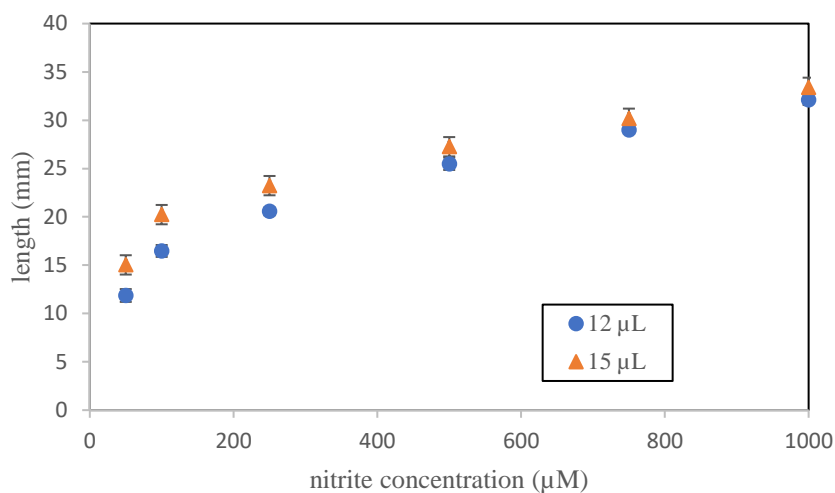


Figure 4.6 Effect of 0.2 M citric acid addition to 5 mM chromotropic acid in 0.1 M sulfuric acid on nitrite detection.

4.1.5 Interference studies

In this work, the effect of potentially interfering species commonly found in samples (water, vegetables, and processed meat) was investigated. The tolerance limit in a solution containing 75 μM nitrite is shown in Table 4.2.

Table 4.2 The tolerance limit of interference species in the detection of 75 μM nitrite

Interference species	Tolerance limit (μM)
NaCl	>50,000
NaNO ₃	>50,000
NaHCO ₃	2,500
KCl	>50,000
CH ₃ COONH ₄	7,500

The tolerance limit is the highest concentration of interfering species present in a nitrite solution as a binary mixture that does not significantly affect the color band length compared to the results in the absence of these species. Apparently, the method could tolerate the presence of these salts starting from 2,500 μM and higher. It should be noted that the color of the band was more intense in the presence of these salts. This could be explained that the diazonium ions on the thread were stabilized by the ions from salts, as a result, the coupling reaction could occur on each specific area of thread to a greater extent. However, the band length remained unchanged. It was also observed that the basic salts including NaHCO_3 and $\text{CH}_3\text{COONH}_4$ strongly affected the detection of nitrite. It was probable that these basic salts would change the pH value on the thread resulting in the unfavorable condition for diazotization reaction to take place. This indicated that the addition of citric acid is necessary in this method. These tolerant levels revealed that the method can be applied to detect nitrite in the above-mentioned samples.

4.1.6 Method validation and sample analysis

Under the chosen conditions, the linear relationship between the thread length and nitrite concentration was obtained in the concentration range of 50 – 1,000 μM as shown in Figure 4.7.

. The photographs of the thread platform are also shown in Figure 4.8. The linear calibration curve could be divided into two ranges of concentration based on the detection sensitivity. The first concentration range was from 50-100 μM nitrite with a linear relationship of $y = 0.104x + 9.698$ ($R^2 = 0.992$), while the second range was from 100 to 1,000 μM nitrite with a linear relationship of $y = 0.0144x + 19.388$ ($R^2 = 0.991$). The relative standard deviation (RSD) of the calibration curves slope did not

exceed 10% when repeated intra-day. Compared to the work of Nilghaz *et al* [39], the same linear range was obtained in this work but with the determination of nitrite as low as 50 μM in this work. The lowest concentration that could produce observable color on the platform was 25 μM . At this concentration, the pale pink color was only observed on the knot at the center of the thread.

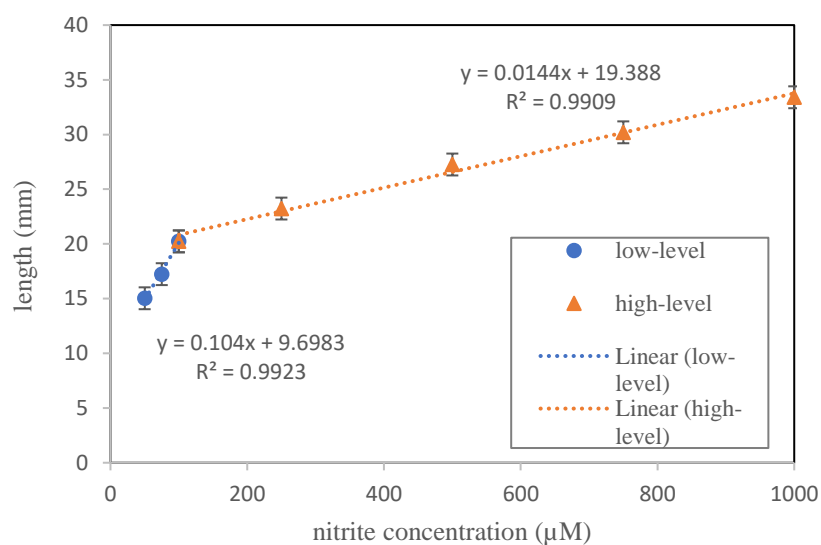


Figure 4.7 Calibration curve for nitrite determination by thread-based platform using reagent solution containing 0.2 M citric acid and 5 mM chromotropic acid in 0.10 M sulfuric acid with 5-time sample introduction (15 μL).



Figure 4.8 The photographs of the thread platform.

According to Figure 4.8, an unequal distribution of color band was observed in the detection of nitrite at high concentration, partly because the volume of 15 μL ($3 \mu\text{L} \times 5$ times) was close to the limit of liquid capacity of the thread. After introducing solution many times, the thread may act like a reservoir containing aqueous solution. Therefore, nitrite ions at high concentration may freely diffuse along the thread and diazotization would not occur periodically. Under the optimum conditions, the calibration curve and response were reproducible, indicating a robustness of the method.

The platform was further used to determine the level of nitrite in various samples. As shown in Table 4.3, the concentrations of nitrite in different samples determined by the thread-based platform were close to the results from ion chromatography method. However, the results from both methods were significantly different at a 95% confidential level especially the results from sausage and Chinese cabbage. The reagent used in sample preparation, especially borax may affect the analysis using ion chromatography. In ion chromatography method, the found concentration was higher than the spiked level because borate ion from borax could interfere the conductivity of nitrite ions. However, the size of standard deviation was small due to the cancellation of electronic signal from a detector when repeated the analysis of the same sample. Although the deviations of the results from the thread-based method were relatively high, the platform still showed robustness in nitrite determination despite different sample matrices.

Table 4.3 Sample analysis and recovery percentage of spiked samples determined by the thread-based platform

Sample	Added (μM)	Thread-based Method			Ion Chromatography method		
		Found ^a (μM)	Recovery (%)	RSD (%)	Found ^a (μM)	Recovery (%)	RSD (%)
Drinking water	0	nd ^c	-	-	nd ^b	-	-
	300	297.5	99.2	6.04	322.6	107.5	1.19
	700	646.8	92.4	4.34	713.9	102.0	0.21
Chinese cabbage	0	nd ^c	-	-	nd ^b	-	-
	300	320.3	106.8	10.43	334.3	111.4	0.71
	700	657.9	94.0	9.04	723.4	103.3	1.43
Sausage	0	75.2	-	7.48	85.3	-	16.16
	300	421.3	115.4	9.99	382.6	99.1	0.36
	700	820.8	106.5	5.26	730.6	92.2	0.48

^a average of triplication

^b detection limit of ion chromatography was 0.72 μM

^c lowest concentration determined by the thread-based platform was 50 μM

The accuracy of the method was evaluated by comparing the results to those obtained by an ion chromatography method and the recovery of nitrite in spiked samples. The results with percentage recovery in the range of 92.4 – 115.4 % was observed using the proposed platform, compared to 92.2 – 111.4 % by ion chromatography method. Relative standard deviation (% RSD) of the results represented the precision of the proposed method was in the range of 4.34 – 10.43 %, compared to 0.21 – 16.16 % by ion chromatography. The results reveal that this

method produced results with acceptable accuracy and precision, recommended in the AOAC recommended in the AOAC International criteria (Table 4.4) [43].

Table 4.4 Acceptable values of analyte recovery and precision (%RSD) for the determination of analyte at different concentrations [43]

Unit	Mean recovery (%)	RSD (%)
100 ppm	90-107	5.3
10 ppm	80-110	7.3
1 ppm	80-110	11
100 ppb	80-110	15
10 ppb	60-115	21
1 ppb	40-120	30

4.2 Determination of nitrite by paper-based platform

4.2.1 Characterization

To prepare the paper platform, the surface of cellulose paper was modified in two steps (Figure 3.2) similar to the session 4.1.1. The hydroxyl groups on cellulose was substituted by *p*-nitrobenzoyl chloride resulting in *p*-nitrobenzoyl-paper that was further reduced to *p*-aminobenzoyl-paper. The obtained materials were characterized by different techniques.

The ninhydrin test was performed on a piece of unmodified filter paper and a piece of *p*-aminobenzoyl-paper to observe primary amine groups. The positive result was observed on *p*-aminobenzoyl-paper as the paper turned purple, while the unmodified filter paper color remained the same. This result confirmed the presence of primary amine group on the modified paper resulted from the surface modification with *p*-aminobenzoyl moiety.

The materials were further characterized by Raman spectroscopy as shown in Figure 4.9 and Table 4.5 [41]. The signal in the Raman spectrum of the unmodified cellulose paper exhibited two peaks at $1,094\text{ cm}^{-1}$ and $1,117\text{ cm}^{-1}$ attributed to the C-O stretching of glycosidic link or C-OH in cellulose. Moreover, the peak at $1,472\text{ cm}^{-1}$ could be assigned to the C-H₂ deformation. These peaks were also present in every samples. The additional peak at $1,343\text{ cm}^{-1}$ observed in the Raman spectrum of the *p*-nitrobenzoyl-paper belonged to C-O-C stretching of para-substituted benzoate. In addition, the presence of a symmetric C-NO₂ stretching of aromatic nitro compound at $1,377\text{ cm}^{-1}$ confirmed that the *p*-nitrobenzoyl moiety was successfully attached onto the cellulose skeleton. After the reduction reaction, the signal of N-H deformation of primary amino group additionally appeared at $1,607\text{ cm}^{-1}$, revealing that the reduction of the nitro group to amino group was successfully done. Nevertheless, the signal of

symmetric C-NO₂ stretching of aromatic nitro compound was still present in the Raman spectrum of the *p*-aminobenzoyl-paper. It indicated that all the nitro groups on the paper was not completely reduced.

The spectrum of the modified paper after nitrite detection exhibited the signals of the N=N stretching of the azo bond at 1,408 cm⁻¹ and 1,507 cm⁻¹. Moreover, the signal of the C-N stretching of the carbon adjacent to the azo bond at 1,291 cm⁻¹ became stronger and broader until it overwhelmed the signal at 1,343 cm⁻¹. The additional peak at 1,569 cm⁻¹ could be assigned to aromatic ring chain vibrations. It should be noted that the stronger peak at 1,602 cm⁻¹ was observed in the Raman spectrum of the modified paper after nitrite detection. This signal could represent naphthalene ring stretching vibrations, revealing the attachment of chromotropic acid. These results confirmed that the diazotization occurred on the modified paper surface.

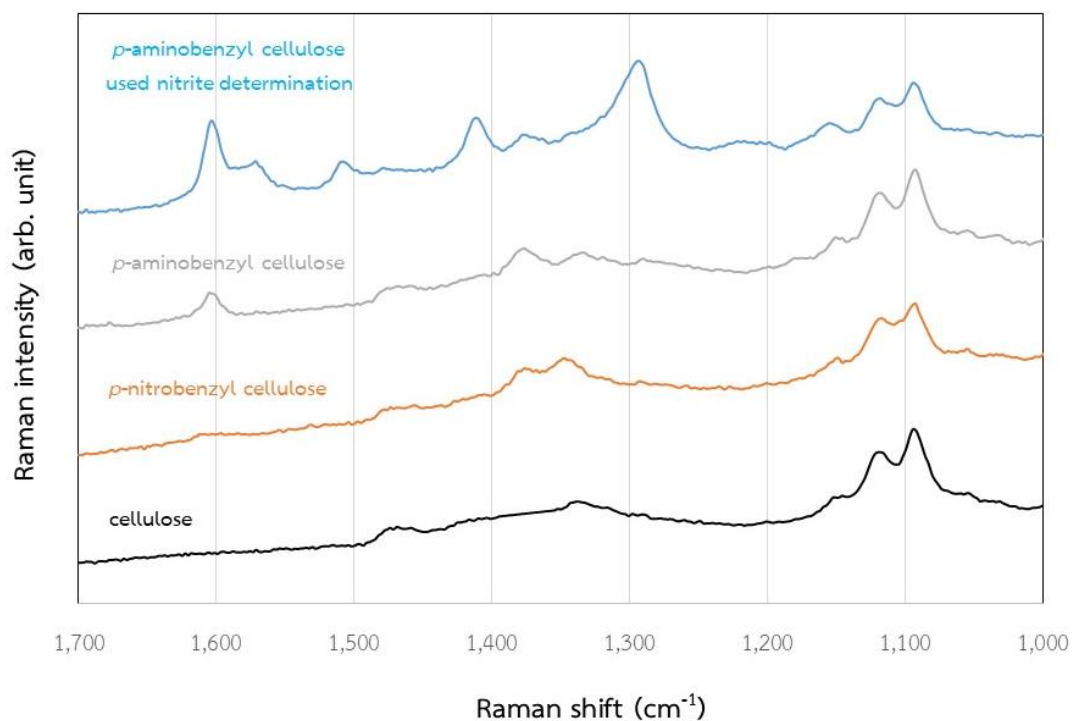


Figure 4.9 Raman spectra of the paper materials.

Table 4.5 Wavenumber and Raman band assignments for paper materials [41]

Material	Functional Groups	Wavenumber (cm ⁻¹)
Unmodified cellulose paper	C-O stretching of C-O-C (glycosidic link) or C-OH in cellulose	1,094
	C-O stretching of C-O-C (glycosidic link) or C-OH in cellulose	1,117
	CH ₂ deformation	1,472
	Additional Functional groups	
<i>p</i> -nitrobenzoyl paper	C-O-C stretching of para-substituted benzoate	1,343
	C-NO ₂ stretching of aromatic nitro compound (symmetric)	1,377
<i>p</i> -aminobenzoyl paper	C-O-C stretching of para-substituted benzoate	1,336
	C-NO ₂ stretching of aromatic nitro compound (symmetric)	1,377
	N-H deformation of primary amino group	1,607
Modified paper after nitrite detection	C-N stretching of carbon adjacent to the azo bond	1,291
	C-NO ₂ stretching of aromatic nitro compound (symmetric)	1,377
	N=N stretching of azo bond	1,408
	N=N stretching of azo bond	1,507
	Aromatic ring chain vibrations	1,569
	Naphthalene ring stretching vibrations	1,602

4.2.2 Effect of *p*-nitrobenzoyl chloride concentration

To obtain the maximum number of amine groups on the paper surface, the effect of *p*-nitrobenzoyl chloride (PNB) amount used in surface modification was investigated. A solution containing 0.01 or 0.02 moles PNB in 100 mL of acetonitrile was used to modify a piece of filter paper (125 mm i.d.). After the surface modification, the obtained papers were cut into circular pieces and used to detect nitrite in solutions containing 0 – 100 μ M nitrite in 0.10 M citric acid. To prevent sample dilution, a small volume of citric acid (200 μ L) was spiked into the sample solution (4.00 mL) to obtain the final citric concentration of 0.10 M. The same procedure was applied in all experiments. The extraction time of 15 minutes was applied. The reagent zone of the paper-based platform was modified with 100 μ M chromotropic acid (10 μ L) for coupling reaction. The experiments were performed in triplicate and the results are shown in Figure 4.10. In the presence of nitrite, the azo dye product was produced on the paper surface and hence, the paper color changed from off-white to pale pink and darker pink in increasing nitrite concentration. The photograph of the paper was taken, and the gray values were collected in Image J program. The results are presented in terms of Δ gray-scale values which were the difference between the gray values of the blank and the paper tested with nitrite solution. The Δ gray-scale values indicated the degree of dye product formation on the paper surface.

It was found that the paper prepared by using 0.01 mole of PNB provided lower Δ gray-scale value when used to detect nitrite solutions, compared to the paper prepared by using 0.02 mole PNB. Moreover, these resulting papers exhibited a non-homogeneous dye color on the surface, revealing that the paper surface was not fully covered with *p*-aminobenzoyl moieties. Therefore, 0.02 mole PNB in 100 mL acetonitrile was chosen to modify the paper surface.

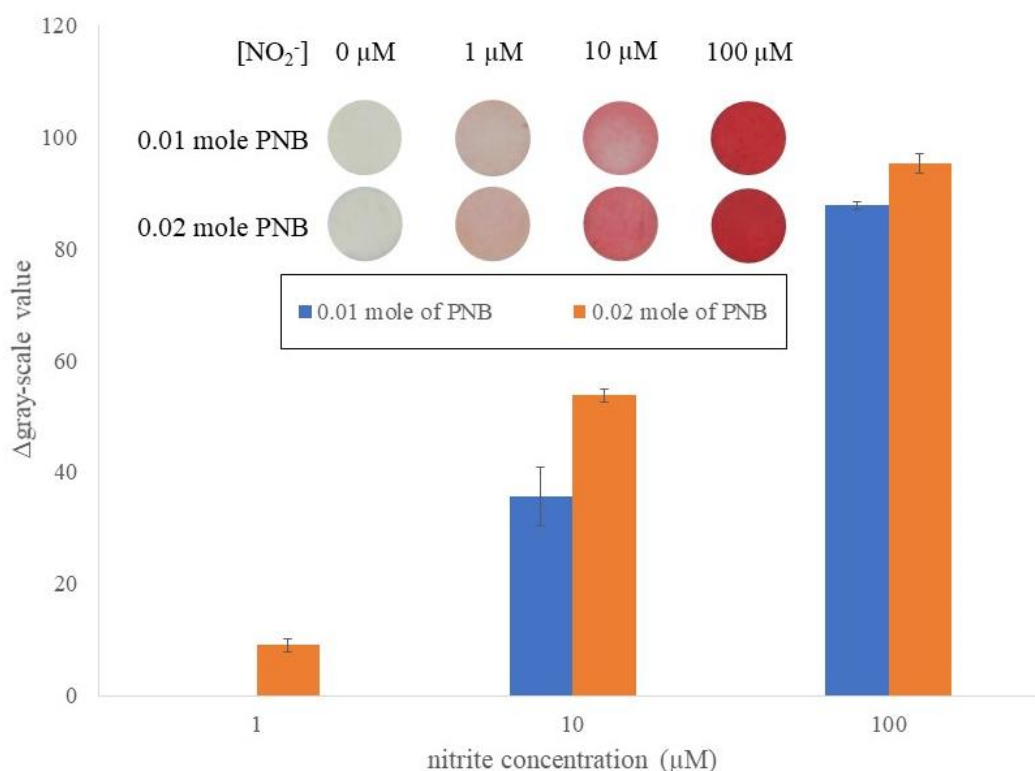


Figure 4.10 Effect of *p*-nitrobenzoyl chloride (PNB) amount used in the paper surface modification in the detection of nitrite (inset – photographs of the papers).

4.2.3 Effect of citric acid concentration

Citric acid was utilized to acidify the nitrite standard and sample solution. In the diazotization reaction, nitrite could be turned to a more reactive intermediate under acidic condition that reacted easily with aromatic amine group to produce diazonium ions. The azo dye product was obtained from the coupling reaction between the diazonium ion and the coupling reagent. In this experiment, the concentration of citric acid was varied in a range from 0.05 to 0.20 M. The other condition for nitrite detection (0 – 20 μM) was kept as 3-mL sample volume, 15-minute extraction time, and 100-μM CTA (10 μL) modified in the reagent zone. As shown in Figure 4.11, citric acid at high concentration provided high ΔGray-scale value. The high

concentration of citric acid increased the reaction rate of nitrite into intermediate that provided high amount of product (red color onto the paper). However, the trend of citric acid at 0.10 M and 0.20 M did not give remarkably different results, citric acid of 0.20 M was chosen for the next experiment to reduce the effect of basic species in samples.



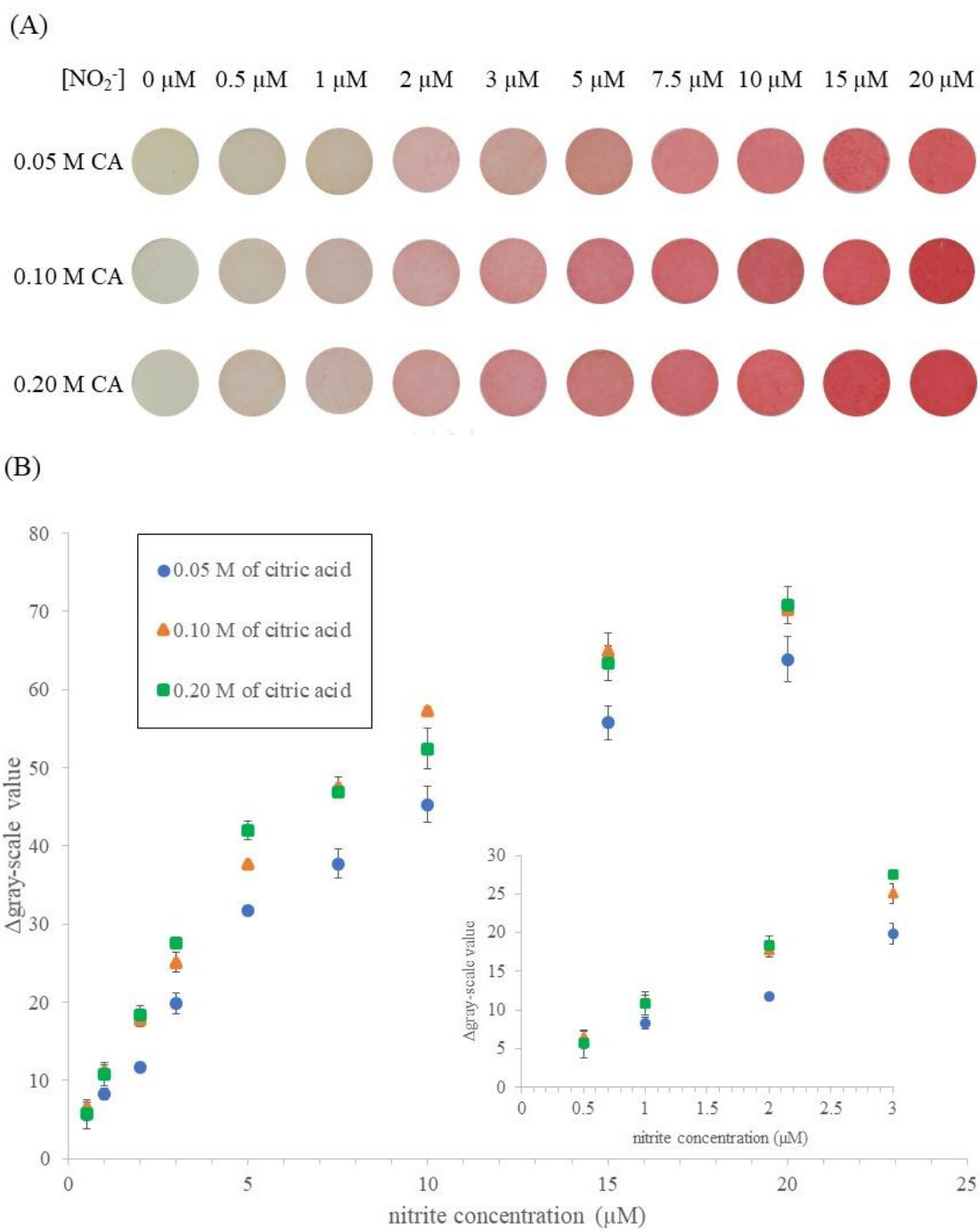


Figure 4.11 Effect of citric acid (CA) concentration in the detection of nitrite ion (A) photograph of testing papers and (B) the effect of citric acid concentration on the observed gray intensities (inset – effect on the detection at low nitrite concentrations).

4.2.4 Effect of sample volume

The effect of sample volume was investigated by varying the sample volume in a range from 1.00 – 4.00 mL. In this experiment, only nitrite ion standard solution was employed to represent the real sample. A 15-minute nitrite extraction time and 100- μ M CTA solution (10 μ L) modified on the reagent zone were applied in the detection of nitrite (0 – 20 μ M). As shown in Figure 4.12, the color intensity slightly increased when the sample volume was increased from 1.00 mL to 3.00 mL. It was found that 3-mL sample volume provided the highest color intensities in the detection of nitrite solutions. However, the color intensity slightly decreased when the sample volume reached to 4.00 mL since the volume was too large for this size of testing paper to stay in contact with the whole solution in limited extraction time. According to our goal to improve the sensitivity of the method by increasing sample volume, the obtained results supported the hypothesis.

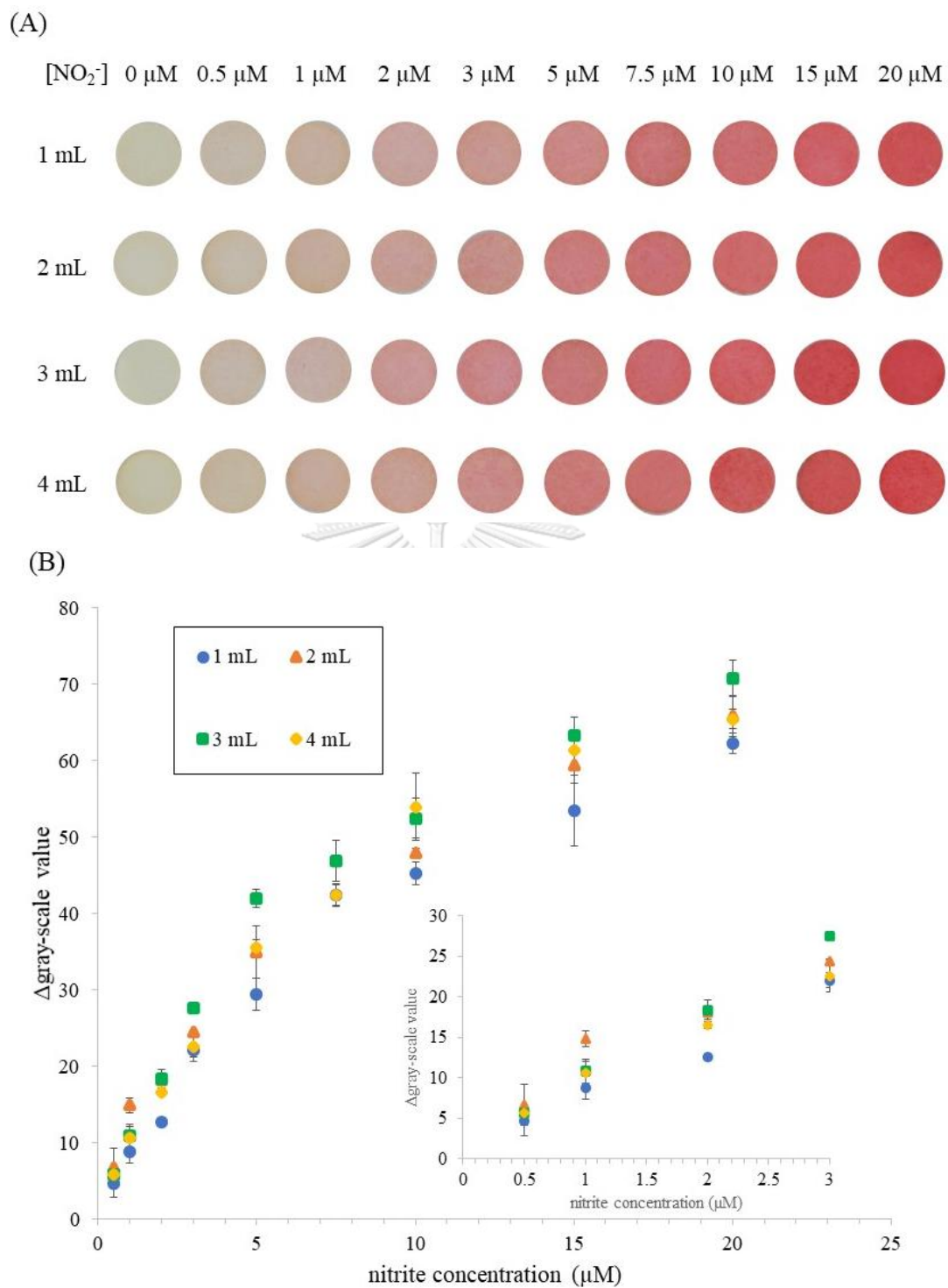


Figure 4.12 Effect of sample volume in the detection of nitrite ion (A) photograph of testing papers and (B) the effect of sample volume on the observed gray intensities (inset – effect on the detection at low nitrite concentrations).

4.2.5 Effect of extraction time

To further improve the detection sensitivity with compromised analytical time, the effect of extraction time was investigated. The time to extract nitrite ions from solution should be long enough for a quantitative amount of nitrite ions to undergo the diazotization reaction on the paper surface. In this experiment, all the previous optimum parameters were used, and the reagent zone was still modified with 100- μ M CTA (10 μ L). As shown in Figure 4.13, it was found that the longer the extraction time, the higher the color intensity was achieved especially in the detection of low nitrite concentration. The intensities observed at 15-minute and 20-minute extraction time were slightly different possibly because a large amount of nitrous acid was produced in contact with 0.20 M citric acid for longer extraction time. A specific amount of nitrous acid may further turn to NO and NO₂ gas and released from the solution before diazotization could occur on the paper surface [42]. Apart from this, it was observed that the paper piece became thinner and the surface became corroded when soaked in solution for 20 minutes. Hence the color observed on the paper surface was less intense and not homogeneous. The 15-minute extraction time was selected in this method.

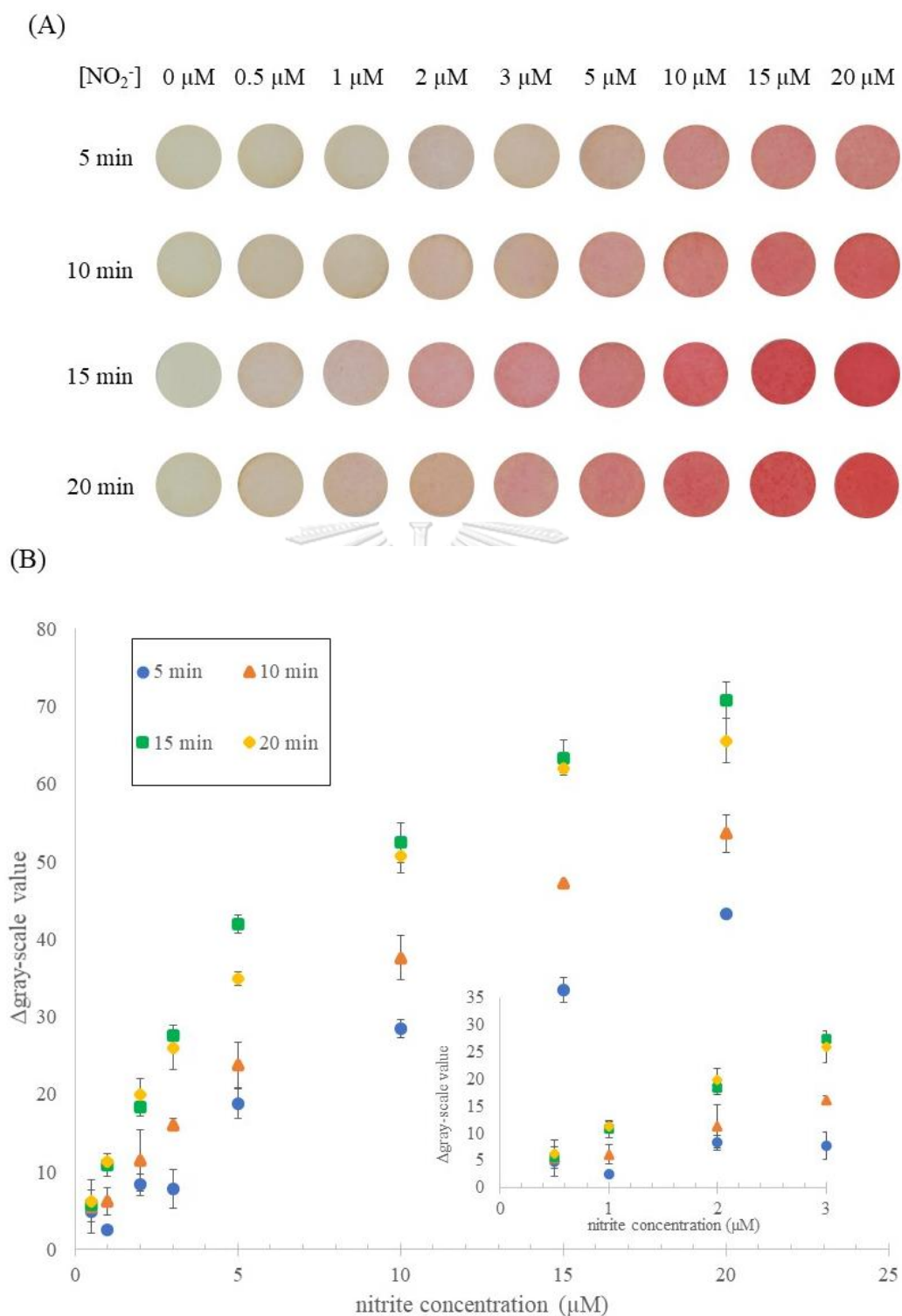
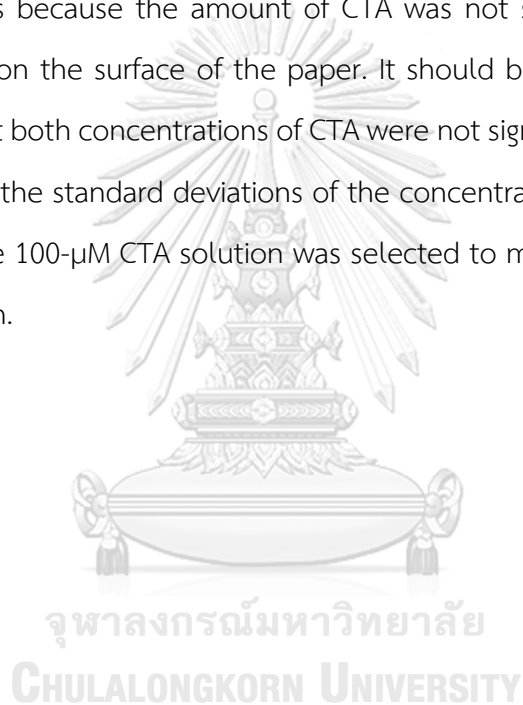


Figure 4.13 Effect of extraction time in the detection of nitrite ion (A) photograph of testing papers and (B) the effect of extraction time on the observed gray intensities (inset – effect on the detection at low nitrite concentrations).

4.2.6 Effect of chromotropic acid concentration

The effect of CTA concentration was investigated to find a suitable concentration to reach a compromise between detection sensitivity and low blank background due to CTA color. The CTA concentration was varied as 50 and 100 μM and the results are shown in Figure 4.14. It was found that there was no difference in Δ gray-scale value when detected nitrite. However, the color on the paper surface using 50 μM CTA was not homogeneous, especially, in the detection of the high nitrite concentration. It is because the amount of CTA was not sufficient to complete the coupling reaction on the surface of the paper. It should be noted that although the results observed at both concentrations of CTA were not significantly different at a 95% confidential level, the standard deviations of the concentration of CTA at 50 μM were relatively high. The 100- μM CTA solution was selected to modify the reagent zone on the paper platform.



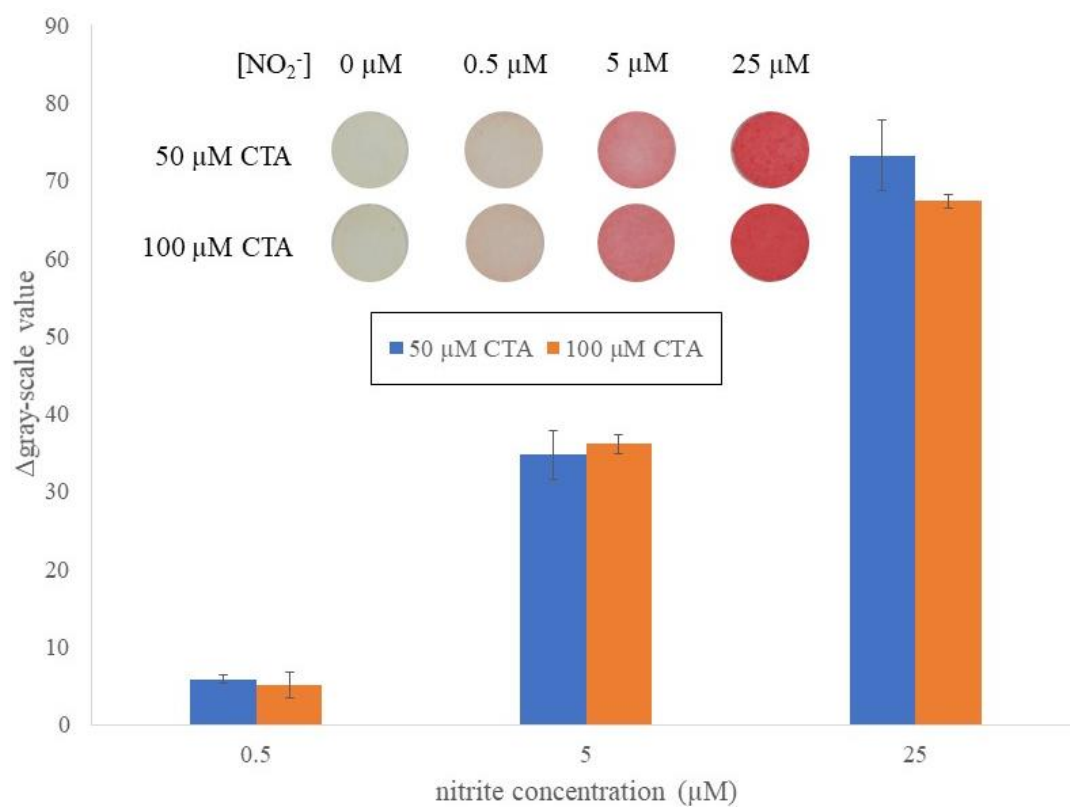


Figure 4.14 Effect of chromotropic acid (CTA) amount used in the reagent zone of the paper-based platform in the detection of nitrite (inset – photographs of the papers).

4.2.7 Interference studies

In this work, the effect of potentially interfering ions commonly found in agricultural runoff was investigated was evaluated. All cations solution was prepared from nitrate salts, while all anion solution was prepared from sodium salts. The tolerance limit of interference ions in the detection of 5 μM nitrite is shown in Table 4.6.

Table 4.6 The tolerance limit of interference ions in the detection of 5 μM nitrite

Interference ions	Tolerance limit (μM)
<u>Cations</u>	
Na^+	25,000
K^+	>40,000
NH_4^+	10,000
Mg^{2+}	10,000
Ca^{2+}	10,000
Fe^{3+}	5,000
<u>Anions</u>	
Cl^-	25,000
NO_3^-	25,000
HCO_3^-	10,000
H_2PO_4^-	25,000
SO_4^{2-}	25,000

In this work, the tolerance limit is defined as the highest concentration of interfering ions present in a nitrite solution as a binary mixture that does not significantly affect the color intensity compared to the results in the absence of these species. Apparently, the method could tolerate the presence of these salts starting from 5,000 μM and higher. It was observed that Fe^{3+} strongly affected the detection of nitrite. However, most agricultural runoff may contain iron in reasonably low level. Consequently, the results revealed that the method can be applied to detect nitrite in the above-mentioned samples.

4.2.8 Method validation and sample analysis

For the determination of nitrite by the paper-based platform, the linear relationship was obtained in the concentration range of 0.5 – 20 μM as shown in Figure 4.15.

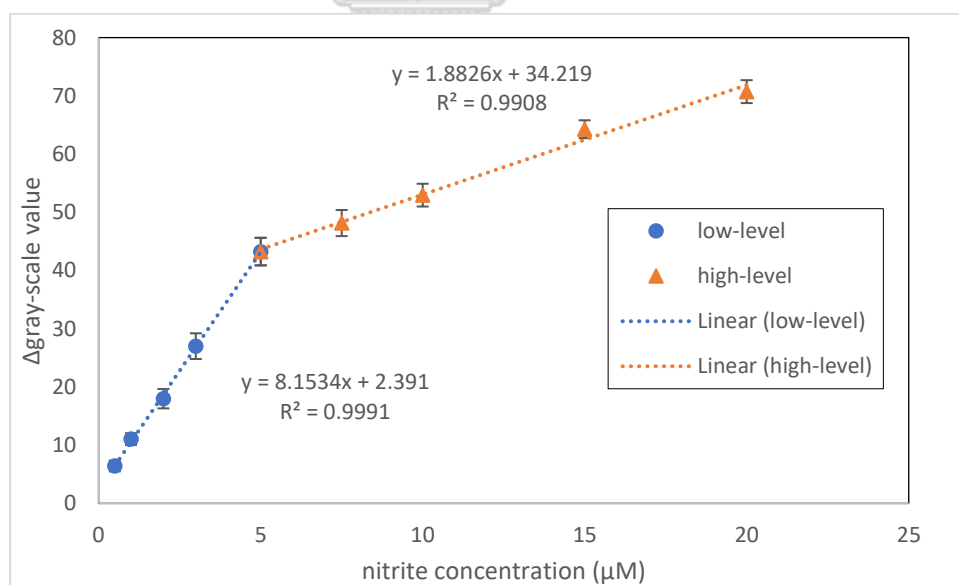


Figure 4.15 Calibration curve for nitrite determination by paper-based platform using 3-mL sample volume in 0.20 M citric acid and 100 μM chromotropic acid in the reagent zone with 15-minute extraction time.

The linear calibration curve could be divided into two ranges of concentration by the difference in detection sensitivity. The first concentration range was from 0.5 - 5 μM nitrite with a linear relationship of $y = 8.1534x + 2.391$ ($R^2 = 0.9991$), while the second range was from 5 to 20 μM nitrite with a linear relationship of $y = 1.8826x + 34.219$ ($R^2 = 0.9908$). The relative standard deviation (RSD) of the calibration curves slope did not exceed 10% when repeated inter-day.

LOD and LOQ for the determination of nitrite ions were calculated to be 0.44 μM and 1.47 μM , respectively. In this work, LOD of this method is the concentration that gave the signal equal to three times of the quotient of the SD for y ($\Delta\text{Gray-scale value}$) estimated over the slope coefficient, while LOQ is the concentration that gave the signal equal to ten times of the quotient of the SD for y ($\Delta\text{Gray-scale value}$) estimated over the slope coefficient.

The platform was further used to determine the level of nitrite in various samples. As shown in Table 4.7, the concentrations of nitrite in different samples determined by the paper-based platform were close to the concentrations determined by ion chromatography method, but the results for spiking at high concentration (*i.e.* 7.5 μM) from both methods were significantly different at a 95% confidential level.

Table 4.7 Sample analysis and recovery percentage of spiked samples determined by the paper-based platform

Sample	Added (μM)	Paper-based Method			Ion Chromatography method		
		Found ^a (μM)	Recovery (%)	RSD (%)	Found ^a (μM)	Recovery (%)	RSD (%)
1	-	3.17	-	7.30	2.58	-	0.81
	2	4.98	90.5	1.04	4.46	94.0	1.60
	7.5	10.64	99.6	2.30	9.28	89.3	0.58
2	-	nd ^c	-	-	nd ^b	-	-
	2	1.93	96.5	7.91	1.69	84.5	1.98
	7.5	6.10	81.3	4.22	7.06	94.1	3.21
3	-	nd ^c	-	-	nd ^b	-	-
	2	1.92	96.0	9.05	1.77	88.5	3.54
	7.5	6.79	90.5	11.69	8.05	107.3	2.67
4	-	nd ^c	-	-	nd ^b	-	-
	2	1.81	90.5	7.33	1.92	96.0	1.44
	7.5	7.76	103.5	9.04	6.61	88.1	2.06
5	-	nd ^c	-	-	nd ^b	-	-
	2	1.93	96.5	8.87	1.91	95.5	6.81
	7.5	7.73	103.1	13.11	6.80	90.7	7.22

^a average of triplication

^b detection limit of ion chromatography was 0.15 μM

^c detection limit determined by the paper-based platform was 0.44 μM

Sample No. 1, 2, 3, 4 and 5 were the runoff from a botanic greenhouse, the water in a paddy field 1, the water in a paddy field 2, the runoff from a paddy field, and the water in a Chinese kale garden, respectively.

The accuracy of the method was evaluated by comparing the results to those obtained by the ion chromatography method and the recovery of nitrite in spiked samples. The proposed platform produced results with percentage recovery in the range of 81.3 - 103.5 %, compared to 84.5 – 107.3 % by ion chromatography method. Percentage of relative standard deviation (% RSD) representing the precision of the proposed method was in the range of 1.04 – 13.1 %, compared to 0.58 – 7.22 % by ion chromatography method. These results confirm that this paper-based method produced results with acceptable accuracy and precision, according to the widely used AOAC criteria summarized in Table 4.4. Furthermore, our platform provided robustness for nitrite determination in the presence of interfering ions.



4.3 Comparison of Method Performance

Comparison of the analytical performance of the developed platforms and other platforms for nitrite detection using the Griess reaction is present in Table 4.8.

Table 4.8 Comparison of the performance of different analytical platforms for nitrite detection using the Griess reaction

Platform	Working range (LOD)	Details	Ref.
Microfluidic paper-based device	10 – 1,000 μM (10 μM)	- Color intensity measurement method - Sample: saliva	[37]
Microfluidic paper-based device	10 – 150 μM (1 μM)	- Color intensity measurement method - Sample: synthetic and natural water - Also applicable to nitrate detection	[36]
Thread-based device	0 – 1,000 μM (ca 100 μM)	- Length measurement method - Test in aqueous solution	[39]
Microfluidic paper-based device	4 – 85 mg/L (0.52 mg/L)	- Color intensity measurement method - Test in aqueous solution - Simultaneous nitrite and pH determination	[38]
Microfluidic cloth-based device	0 – 500 μM (30 μM) ^a	- Color intensity measurement method - Sample: urine - Simultaneous nitrite, glucose, and protein determination	[44]

Table 4.8 Comparison of the performance of different analytical platforms for nitrite detection using the Griess reaction (*cont.*)

Platform	Working range (LOD)	Details	Ref.
Microfluidic paper-based device	0 – 25 μM (5.6 μM)	<ul style="list-style-type: none"> - Color intensity measurement method - Sample: saliva, food, and river water - Applicable to the preconcentration step on the device before introducing the Griess reagent 	[45]
Cotton fiber-based assay	0 – 300 μM (6.56 μM)	<ul style="list-style-type: none"> - Color intensity measurement method - Sample: artificial saliva - Microfluidic absorption sampling 	[46]
Paper-based device	0.5 – 1,000 mg/L (0.1 mg/L and 0.15 mg/L) ^b	<ul style="list-style-type: none"> - Color intensity measurement method - Sample: food - Using chemometrics to construct the calculation models 	[47]
Paper-based device	1 – 250 mg/kg ^c (1.1 mg/kg)	<ul style="list-style-type: none"> - Color intensity measurement method - Sample: food - Using the coffee-ring effect to enhance the performance 	[48]
Microfluidic paper-based device	1 – 100 mg/L (1 mg/L)	<ul style="list-style-type: none"> - Color intensity measurement method - Sample: food 	[49]
Paper-based device	0.40 - 20 mg/L (0.40 mg/L)	<ul style="list-style-type: none"> - Color intensity measurement method - Sample: food - Simultaneous nitrite, nitrate, borax, and salicylic acid determination 	[50]

Table 4.8 Comparison of the performance of different analytical platforms for nitrite detection using the Griess reaction (*cont.*)

Platform	Working range (LOD)	Details	Ref.
Thread-based device	50 – 1,000 μM (25 μM) ^a	<ul style="list-style-type: none"> - Length measurement method - Sample: food and drinking water - Chemically <i>p</i>-aminobenzoyl moiety on the thread surface with chromotropic acid impregnation 	This work
Paper-based device	0.5 – 20 μM (0.44 μM)	<ul style="list-style-type: none"> - Color intensity measurement method - Sample: agricultural runoff - Chemically <i>p</i>-aminobenzoyl moiety on the surface and using chromotropic acid as coupling reagent 	This work

^a Lowest concentration that could be detected

^b Proposed by two different mathematical models

^c Using a logarithmic curve

The proposed thread-based and the paper-based devices showed an analytical performance that was comparable to previously reported work.

For the thread-based platform, increasing the sample volume could lower the detection limit compared to the thread based platform proposed by Nilghaz *et al.* [39]. Furthermore, the distinct advantage was the robustness of the method in the presence of interfering species. Although the color intensity of produced dyes along the threads in the absence and in the presence of these species was completely different, the length of color band remained the same. This indicates that the thread-based device could be employed for nitrite determination in complex sample matrices such as food samples.

For the paper-based platform, the nitrite at trace level could be detected because the sample size was raised to milliliter level. Moreover, the prominence was that the extraction of nitrite ions from the sample matrix could be done. The effect of interfering species in real samples was minimized.

Consequently, these platforms could be potentially applied to detect trace levels of nitrite found in various samples including foods, biological samples (*e.g.* saliva and urine), and water samples with robustness and acceptable accuracy and precision.



CHAPTER V

CONCLUSIONS

5.1 Conclusions

The thread-based device and the paper-based device for the colorimetric determination of nitrite ions based on Griess reaction were successfully developed. The materials surface was chemically modified with *p*-aminobenzoyl moiety and CTA was used as a coupling reagent. The detection of nitrite was achieved by measuring the color band length in case of the thread-based device and color intensity in the case of the paper-based device.

Considering the initial hypothesis that the thread surface modification would decrease the unequal distribution of the reagents, it was found that the color on the thread still appeared unequally at high nitrite concentration. However, the generation of diazonium ions directly on the material surface could contribute many advantages including increasing sample size and the elimination of interference effect. Under the optimum condition, the devices were employed to determine nitrite ions in various kinds of real samples. The devices not only produced results with acceptable accuracy and precision, but also provided the robustness in nitrite detection in the presence of potential interfering species. The parameters affecting the determination of nitrite ions using the devices were optimized. The optimum conditions using the thread-based device and the paper-based device are shown in Table 5.1 and Table 5.2, respectively.

The lowest concentration that could be detected for the determination of nitrite ions using the thread-based device was 25 μM . On the other hand, LOD and

LOQ for the determination of nitrite ions using the paper-based device were 0.44 μM and 1.47 μM , respectively.

Table 5.1 The optimum conditions using the thread-based device

Parameters	Optimum conditions
CTA concentration	5 mM
Sulfuric acid concentration	0.10 M
CA concentration	0.2 M
Sample volume	15 μL with a 3-minute time interval

Table 5.2 The optimum conditions using the paper-based device

Parameters	Optimum conditions
CTA concentration	100 μM
CA concentration	0.20 M
Sample volume	3.00 mL
Extraction time	15 minutes

5.2 Suggestions for future work

The shelf life of the materials should be investigated. The stability test of the modified thread impregnated CTA and the stability of CTA on the reagent zone in the paper-based platform should be evaluated. In addition, other cellulose-based materials can be further developed with the same concept to detect nitrite ion in other kind of samples.

REFERENCES

1. Van Cleemput, O. and A.H. Samater, *Nitrite in soils: accumulation and role in the formation of gaseous N compounds*. Fertilizer research, 1995. **45**(1): p. 81-89.
2. Afkhami, A., S. Masahi, and M. Bahram, *Spectrophotometric Determination of Nitrite Based on Its Reaction with p-Nitroaniline in the Presence of Diphenylamine in Micellar Media*. Bulletin of the Korean Chemical Society, 2004. **25**(7): p. 1009-1011.
3. Reddy, D., J. Lancaster, and D. Cornforth, *Nitrite inhibition of Clostridium botulinum: electron spin resonance detection of iron-nitric oxide complexes*. Science (New York, N.Y.), 1983. **221**: p. 769-70.
4. Santamaria, P., *Nitrate in vegetables: toxicity, content, intake and EC regulation*. Journal of the Science of Food and Agriculture, 2006. **86**(1): p. 10-17.
5. Lee, D.H.K., *Nitrates, nitrites, and methemoglobinemia*. Environmental Research, 1970. **3**(5): p. 484-511.
6. Chan, T.Y.K., *Food-borne nitrates and nitrites as a cause of methemoglobinemia*. Southeast Asian Journal of Tropical Medicine and Public Health, 1996. **27**(1): p. 189-192.
7. Fahey, J.M. and I. Robert L, *Pretreatment effects on nitrite-induced methemoglobinemia: Saline and calcium channel antagonists*. Pharmacology Biochemistry and Behavior, 1990. **37**(3): p. 457-459.
8. Hegesh, E. and J. Shiloah, *Blood nitrates and infantile methemoglobinemia*. Clinica Chimica Acta, 1982. **125**(2): p. 107-115.
9. Bartsch, H., *N-nitroso compounds and human cancer: where do we stand?* IARC Sci Publ, 1991(105): p. 1-10.
10. Knobloch, L., et al., *Blue babies and nitrate-contaminated well water*. Environmental health perspectives, 2000. **108**(7): p. 675-678.
11. Butler, A., *Nitrites and nitrates in the human diet: Carcinogens or beneficial hypotensive agents?* Journal of Ethnopharmacology, 2015. **167**: p. 105-107.

12. Olajos, E.J. and F. Coulston, *Comparative toxicology of N-nitroso compounds and their carcinogenic potential to man*. *Ecotoxicology and Environmental Safety*, 1978. **2**(3): p. 317-367.
13. Lijinsky, W. and S.S. Epstein, *Nitrosamines as Environmental Carcinogens*. *Nature*, 1970. **225**(5227): p. 21-23.
14. Santarelli, R.L., F. Pierre, and D.E. Corpet, *Processed Meat and Colorectal Cancer: A Review of Epidemiologic and Experimental Evidence*. *Nutrition and Cancer*, 2008. **60**(2): p. 131-144.
15. Wang, Q.-H., et al., *Methods for the detection and determination of nitrite and nitrate: A review*. *Talanta*, 2017. **165**: p. 709-720.
16. Morales, J.A., L.S. de Graterol, and J. Mesa, *Determination of chloride, sulfate and nitrate in groundwater samples by ion chromatography*. *Journal of Chromatography A*, 2000. **884**(1): p. 185-190.
17. Kubáň, P., P. Kubáň, and V. Kubáň, *Capillary electrophoretic determination of inorganic anions in the drainage and surface water samples*. *Journal of Chromatography A*, 1999. **848**(1): p. 545-551.
18. Badea, M., et al., *New electrochemical sensors for detection of nitrites and nitrates*. *Journal of Electroanalytical Chemistry*, 2001. **509**(1): p. 66-72.
19. Jie, S., et al., *Measurement of Nitric Oxide Production in Biological Systems by Using Griess Reaction Assay*. *Sensors*, 2003. **3**.
20. Deng, T., et al., *An unexpected Griess reaction on the important anti-malarial drug primaquine and its application for drug determination*. *Journal of Pharmaceutical and Biomedical Analysis*, 2019. **171**: p. 8-14.
21. Laue, W., et al., *Nitrates and Nitrites*, in *Ullmann's Encyclopedia of Industrial Chemistry*. 2000.
22. Du, S.-t., Y.-s. Zhang, and X.-y. Lin, *Accumulation of Nitrate in Vegetables and Its Possible Implications to Human Health*. *Agricultural Sciences in China*, 2007. **6**(10): p. 1246-1255.

23. Macdougall, D.B., D.S. Mottram, and D.N. Rhodes, *Contribution of nitrite and nitrate to the colour and flavour of cured meats*. *Journal of the Science of Food and Agriculture*, 1975. **26**(11): p. 1743-1754.
24. Froehlich, D.A., E.A. Gullett, and W.R. Osborne, *Effect of Nitrite and Salt on the Color, Flavor and Overall Acceptability of Ham*. *Journal of Food Science*, 1983. **48**(1): p. 152-154.
25. Turrini, A., A. Saba, and C. Lintas, *Study of the italian reference diet for monitoring food constituents and contaminants*. *Nutrition Research*, 1991. **11**(8): p. 861-873.
26. Gangolli, S.D., et al., *Nitrate, nitrite and N-nitroso compounds*. *European Journal of Pharmacology: Environmental Toxicology and Pharmacology*, 1994. **292**(1): p. 1-38.
27. Bedale, W., J.J. Sindelar, and A.L. Milkowski, *Dietary nitrate and nitrite: Benefits, risks, and evolving perceptions*. *Meat Sci*, 2016. **120**: p. 85-92.
28. *Quality recommendation criteria for water*. 2020 [cited 2020 September, 9]; Available from: http://foods.anamai.moph.go.th/ewt_dl_link.php?nid=4112&filename=water_index18.
29. *Quality criteria for drinking tap water*. 2020 [cited 2020 September, 9]; Available from: http://foods.anamai.moph.go.th/ewt_dl_link.php?nid=4113&filename=water_index18.
30. *Food additives*. 2012 [cited 2020 September, 8]; Available from: <http://food.fda.moph.go.th/data/tradermain/Update%20Food%20Additives2-2556.pdf>.
31. Regitz, M. and G. Maas, *Chapter 5 - Diazotization of Amines*, in *Diazo Compounds*, M. Regitz and G. Maas, Editors. 1986, Academic Press. p. 201-220.
32. Griess, P., *Bemerkungen zu der Abhandlung der HH. Weselsky und Benedikt „Ueber einige Azoverbindungen“*. *Berichte der deutschen chemischen Gesellschaft*, 1879. **12**(1): p. 426-428.

33. Bratton, A.C., E.K. Marshall, and A.R. Hendrickson. *A NEW COUPLING COMPONENT FOR SULFANILAMIDE DETERMINATION*. 1939.
34. Seikel, M.K., *Oxidation Products of Sulfanilamide*. Journal of the American Chemical Society, 1940. **62**(5): p. 1214-1216.
35. *Bioassay of N-(1-naphthyl)ethylenediamine dihydrochloride for possible carcinogenicity*. Natl Cancer Inst Carcinog Tech Rep Ser, 1979. **168**: p. 1-103.
36. Jayawardane, B.M., et al., *Microfluidic Paper-Based Analytical Device for the Determination of Nitrite and Nitrate*. Analytical Chemistry, 2014. **86**(15): p. 7274-7279.
37. Bhakta, S.A., et al., *Determination of nitrite in saliva using microfluidic paper-based analytical devices*. Analytica Chimica Acta, 2014. **809**: p. 117-122.
38. Lopez-Ruiz, N., et al., *Smartphone-Based Simultaneous pH and Nitrite Colorimetric Determination for Paper Microfluidic Devices*. Analytical Chemistry, 2014. **86**(19): p. 9554-9562.
39. Nilghaz, A., et al., *Semiquantitative analysis on microfluidic thread-based analytical devices by ruler*. Sensors and Actuators B: Chemical, 2014. **191**: p. 586-594.
40. *National Food Safety Standard Determination of Nitrite and Nitrate in Foods*. GB 5009.33-2016 2016 [cited 2020 September, 8]; Available from: www.chinesestandard.net.
41. Larkin, P.J., *Infrared and Raman Spectroscopy: Principles and Spectral Interpretation*. 2011: Elsevier.
42. Braida, W. and S.K. Ong, *Decomposition of Nitrite Under Various pH and Aeration Conditions*. Water, Air, and Soil Pollution, 2000. **118**(1): p. 13-26.
43. AOAC International, *Guidelines for Standard Method Performance Requirements AOAC Official Methods of Analysis*. , in *Appendix F*. 2016. p. 1-18.
44. Nilghaz, A., et al., *Multiple semi-quantitative colorimetric assays in compact embeddable microfluidic cloth-based analytical device (μ CAD) for effective point-of-care diagnostic*. Microfluidics and Nanofluidics, 2015. **19**(2): p. 317-333.

45. Cardoso, T.M.G., P.T. Garcia, and W.K.T. Coltro, *Colorimetric determination of nitrite in clinical, food and environmental samples using microfluidic devices stamped in paper platforms*. Analytical Methods, 2015. **7**(17): p. 7311-7317.
46. Wicaksono, D.H., et al., *Cotton fiber-based assay with time-based microfluidic absorption sampling for point-of-care applications*. Bioanalysis, 2019. **11**(9): p. 855-873.
47. Almasvandi, Z., *Coupling of digital image processing and three-way calibration to assist a paper-based sensor for determination of nitrite in food samples*. RSC advances, 2020. **v. 10**(no. 24): p. pp. 14422-14430-2020 v.10 no.24.
48. Trofimchuk, E., et al., *Development of paper-based microfluidic device for the determination of nitrite in meat*. Food Chemistry, 2020. **316**: p. 126396.
49. Hou, C.-Y., et al., *Microfluidic colorimetric system for nitrite detection in foods*. Chemical Engineering Journal, 2020. **398**: p. 125573.
50. Ratnarathorn, N. and W. Dungchai, *Paper-based Analytical Device (PAD) for the Determination of Borax, Salicylic Acid, Nitrite, and Nitrate by Colorimetric Methods*. Journal of Analytical Chemistry, 2020. **75**: p. 487-494.



จุฬาลงกรณ์มหาวิทยาลัย
CHULALONGKORN UNIVERSITY

VITA

NAME Mr.Pitcha Singhaphan

DATE OF BIRTH 7 October 1988

PLACE OF BIRTH Trat, Thailand

INSTITUTIONS ATTENDED Department of Chemistry, Faculty of Science,
Chulalongkorn University

HOME ADDRESS 13/8 Chaimongkol Road, Bangphra, Mueang Trat District,
Trat, Thailand

